

AN ABSOLUTE CALORIMETER FOR THE
MEASUREMENT OF HIGH RADIATION FLUX

by

Charles Edwin Neal

Thesis submitted to the Graduate Faculty of the
Virginia Polytechnic Institute
in candidacy for the degree of

MASTER OF SCIENCE

in

MECHANICAL ENGINEERING

June, 1960

Blacksburg, Virginia

TABLE OF CONTENTS

	<u>Page</u>
LIST OF FIGURES	5
LIST OF TABLES	7
I. INTRODUCTION	8
II. REVIEW OF LITERATURE	11
The Production of High Temperatures	11
The Production of High Temperatures by Plasma Generation	11
A. Magnetic Acceleration Method	11
B. Electronic Torch Method	14
The Production of High Temperatures by High Pressure Discharge	16
The Production of High Temperatures by Combustion Furnaces	17
The Production of High Temperatures by Electric Furnaces	18
The Production of High Temperatures by Solar Furnaces	20
The Production of High Temperatures by Direct-Current Arc Furnaces	24
Previous Methods of Determining the Emissivity or Emittance of a Surface	30
Hutchins' Method	30
Royd's Method and Coblentz's Method	31
Nutting's Method	34
Wilkes' Method	34
Schmidt's Method	36
Dobbin's Method	39

Dunkle and Gier's Method	44
Aref's Method	45
Metzger's Method	48
Incandescent Temperature Measurement	53
Thermocouples	53
Radiation Pyrometers	56
A - Optical Pyrometers	56
B - Total Radiation Pyrometers	58
C - Photoelectric Pyrometers	59
D - Radiometers	60
Calorimeters	61
III. THE INVESTIGATION	65
Object	65
Design of Calorimeter	65
Reflector	65
Receiver	69
Cooling Coil	74
Insulation	76
List of Apparatus	78
Operating Apparatus	78
Testing Apparatus	78
Tested Apparatus	79
Operational Procedure	81
Data and Results	88
Receiver Test Series	88

Reflector Test Series	88
Flux Distribution Test Series	90
IV. SAMPLE COMPUTATIONS	94
V. DISCUSSION	97
Receiver Test Series	97
Reflector Test Series	99
Flux Distribution Test Series	99
Other Pertinent Information From all Test Series .	103
VI. CONCLUSIONS	107
VII. RECOMMENDATIONS	108
VIII. ACKNOWLEDGEMENTS	109
IX. BIBLIOGRAPHY	110
X. APPENDIX	113
XI. VITA	121

LIST OF FIGURES

<u>Figure</u>	<u>Page</u>
1. Schematic of Gas Accelerator	13
2. Electronic Torch	15
3. Solar Furnace Schematics	22
4. Free Collector Tracking System	23
5. Fixed Collector Installation	23
6. Adjustable Cylinder-Type Temperature Control For Solar Furnaces and Arc-Image Furnaces	25
7. Schematic of the Formation of the Image, I, of an Object, O, at the Focal Planes of Two Parabolic Reflectors	28
8. Absolute Integrating Radiometer	32
9. Top View of Thermopile and Test Surface Adjustable Stand	33
10. Radiometer	37
11. Schematic of Apparatus for the Determination of Emissivities	38
12. Cross Section of Probe-Type Radiometer	46
13. Schematic of Apparatus for Direct-Comparative Emissivity Study	47
14. Operation of Mechanical Discriminator	51
15. Section Through Miniature Radiometer	62
16. Section Through Absolute Calorimeter	62
17. Brass Calorimeter Reflector	66
17a. Brass Calorimeter Reflector	67
18. Partial Graphical Analysis of Receiver Configuration at 30° and 60° Incident Rays	70

19. Calorimeter Receivers	71
19a. Calorimeter Receivers with Cooling Coil	75
20. Partial Assembly of Calorimeter	77
21. Schematic of Apparatus	82
22. Arc-Image Furnace Flux Distribution as Measured by Calorimeter	101

LIST OF TABLES

<u>Table</u>	<u>Page</u>
1. Receiver Test Series	89
2. Reflector Test Series	91
3. Flux Distribution Test Series	93

I. INTRODUCTION

Today engineers are being confronted with major problems in heat transmission design. This is due primarily to the elevated temperatures which will or could possibly occur during the operation of the device under consideration.

Before 1940, operating temperatures of engines and many, if not all, other devices were far below 1000°F. Today, men are anticipating and witnessing temperatures far over 1000°F.

It is true that in most cases of extremely high temperatures, we are confined mostly to the general field of space vehicles, ballistic missiles, and their propulsion units. It must be realized however that in the near future, devices other than the aforementioned group will need consideration of high temperature heat transmission design.

In heat transmission design, the engineer has at his disposal three modes of heat transmission, these being heat transmission by conduction, heat transmission by convection, and heat transmission by thermal radiation.

For the most part, heat transfer by conduction is of importance in the consideration of bodies in physical contact. In this consideration the factors effecting the quantity of heat transferred are the area of contact, the difference in the temperature of the bodies, and the thermal conductivity of the bodies in question.

In the analysis of heat transfer from a body to a fluid, empirical equations are usually developed and utilized which cover heat transmission due to both conduction of the fluid in contact with the body, and con-

vection of the fluid passing around the body.

In the consideration of heat transmission due to thermal radiation, the engineer must be concerned with the configuration factor for the device and its surrounding media. However, he must be primarily concerned with the emissivity or emittance of the surface of the device in question.

Emissivity can probably be best defined⁽³⁷⁾ as the ratio of the thermal radiation emitted from a perfectly polished surface as a consequence of temperature only, to the thermal radiation emitted from a perfect emitter (which is termed a "blackbody") at the same temperature. Thus, if a surface has an emissivity of 0.5, it would emit only half as much thermal radiation as a "blackbody" at the same temperature. Surfaces or bodies with an emissivity less than 1.0 are termed "graybodies" if their emissivities are constant at all radiation wave lengths.

The emittance of the surface of a body takes into account the deviation of the surface from the perfectly polished condition. It is defined⁽³⁷⁾ as the ratio of the emission of thermal radiation from a body at some temperature, regardless of surface conditions as a consequence of temperature only, to the thermal radiation from a blackbody at the same temperature. Thus the emissivity and the emittance of a perfectly polished surface are numerically equal. If surface becomes corroded, oxidized or highly roughened, the emittance will differ from the emissivity, in most cases the emittance being the greater.

It may be stated, that the suffix "ance" designates extensive or so-called colligative properties, whereas the suffix "ivity" describes only the intensive or non-colligative properties.⁽¹⁰⁾

At this time, engineers have no accurate method of evaluating the

emissivity or emittance of a surface at elevated temperatures. J. W. Metzger⁽²⁸⁾ has recently conducted some research but at the present is dis-satisfied with the results obtained. Therefore, design engineers have available incomplete charts from which values can be very roughly extrapolated for the emissivity or emittance of a surface. This practice is very undesirable because it is well known that some materials exhibit a very noticeable change in emissivity at elevated temperatures, however at the present, it is the only method available.

It can easily be realized that further research should be done in the field of high temperature emissivity and emittance. The measurement of temperature is of major importance in the investigation of emissivity and emittance, therefore, the object of this thesis is the development of a calorimeter which can determine the temperature of the focal plane of an arc-image furnace by measuring the radiation flux at that point.

Since the eventual application of the calorimeter developed in this investigation will be in the study of emissivity and emittance, the following discussion of pertinent literature is included for the benefit of future investigations.

II. REVIEW OF LITERATURE

In presenting a review of the literature pertinent to the investigation of high temperature emissivities and emittances, there are three major subjects which are of primary concern to investigators. These are: (1) the production of high temperatures, (2) previous methods of determining emissivity and (3) the measurement of high temperatures.

A discussion of the literature relative to these topics follows.

The Production of High Temperatures

In order for a study of emissivity and emittance to be conducted at elevated temperatures, there must be available some means of producing the desired temperature. At the present there are several methods⁽³¹⁾ of producing high temperatures, the majority of the most applicable of these being: plasma generation, high pressure discharge, electrical furnace, solar furnace, and direct current arc furnace. Each of these methods will be discussed below.

The Production of High Temperatures by Plasma Generation

A. Magnetic Acceleration Method⁽²⁶⁾

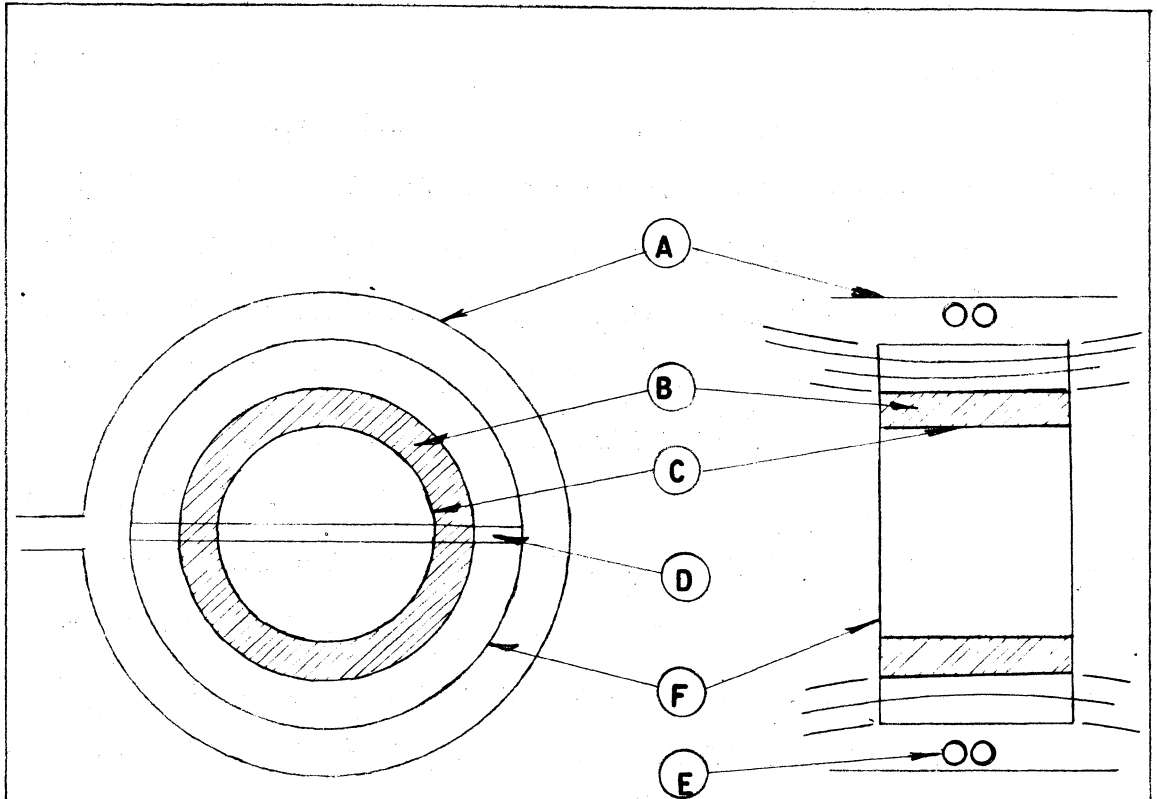
High temperatures can be attained by accelerating gases to high velocities and allowing this energy to be partially randomized by collisions with a fast moving shock front. This is possible because the electrical conductivity of high temperature gas permits the application of forces by means of rapidly changing magnetic fields. Under this condition, a magnetic field discontinuity acts very much like a piston with an applied force per unit area equal to the discontinuity in the magnetic

energy density. One device utilizing this principle is the electrodeless gas accelerator.

This device, as illustrated by Fig. 1, consists of an exterior single turn copper coil whose leads are connected to a capacitor through a pressurized spark gap and a non-linear transmission line. Inside the coil there is a pill box shaped pyrex chamber containing hydrogen or deuterium at a low pressure. This chamber is surrounded by a radio frequency excited preionization coil which is used to provide the initial gas conductivity.

When a voltage is applied to the main coil leads, the induced gas currents are acted upon by the rising magnetic field in such a manner as to produce a rapidly inward accelerating force. Thus a moving slug of hot gas is created while the magnetic field lines tend to be excluded from the center by the electrical gas conductivity. Cold gas ahead of this moving slug should then be heated by collisions which occur during the acceleration process.

This device eliminates electrode surface problems, but has serious other limitations. One of these is the necessity of preionization for reproducible breakdown. Without electrodes, this becomes intrinsically difficult below 50 microns gas pressure. Another difficulty which is basic to all single coil inductive coupling mechanisms has to do with the short range characteristics of the dipole magnetic field. In order to attain conditions of interest to this type research, it is necessary to produce an acceleration field of 12,000 gauss in a time comparable with the maximum gas velocity divided by the chamber radius. This time



- (A) COPPER DRIVE COIL
- (B) HOT GAS
- (C) SHOCK
- (D) SLIT FOR ROTATING MIRROR CAMERA
- (E) PREIONIZATION COIL
- (F) GLASS CHAMBER

Figure 1. SCHEMATIC OF GAS ACCELERATOR

is of the order of 0.25 μ sec.

B. Electronic Torch Method

In an electronic torch or plasma generator, (the term "electronic torch" is sometimes applied to the more conventional term "plasma generator"), high temperatures are produced by the dissociation of molecules of a gas, usually polyatomic, by means of an electrical current.

The most conventional electronic torches are usually powered by a direct current in which the plasma is formed by the passing of the current through a gas to be dissociated between inclined or angular electrodes. When the current passes between the electrodes, dissociating the conducting current, there is a "magnetic pinch" formed by the passing current which increases the density of the plasma and exerts a slight force on the plasma. This force in addition to the pressure of the supply gas, forces the plasma out of the device. This plasma appears as a flame. Usually nozzle arrangements of the electrodes are incorporated to impart higher velocities to the flame. The velocities of torches, using nozzles as stated by J. D. Corbine and D. A. Wilbur⁽⁸⁾, range from 50 to 200 linear-feet per minute.

Alternating currents are sometimes applied in plasma generation. Usually these torches, as illustrated in Fig. 2, are very similar to the direct current torches. In most instances, for suitable production of plasma, frequencies of the a-c current are in the proximity of 1000 megacycles per second.

In reference to the temperatures produced in electronic torches, Corbine and Wilbur further state, "Probe studies of the flame indicate

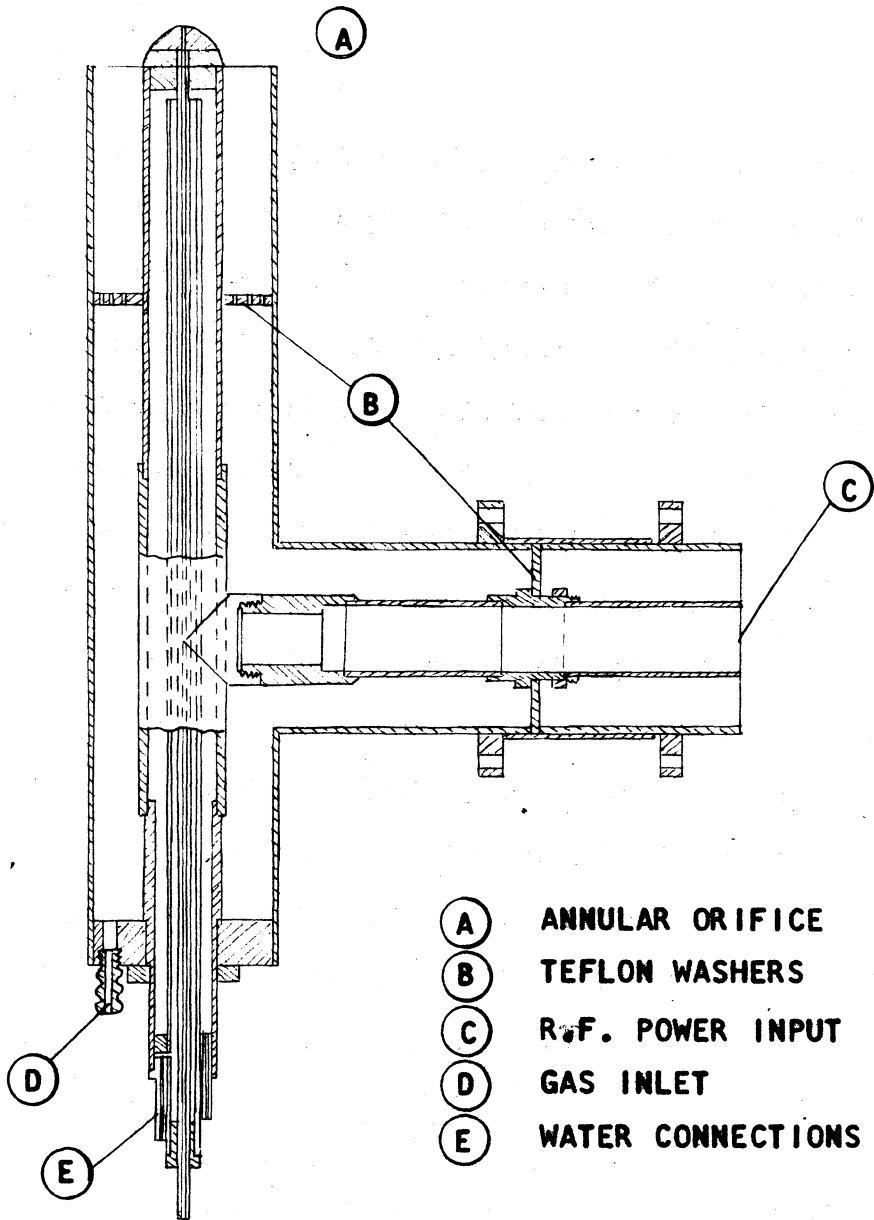


Figure 2. ELECTRONIC TORCH

electron temperatures of from 7.9×10^4 °K at the tip of the flame to 13×10^4 °K near the inner electrode."

At the present time, extensive research has not been conducted with this type of apparatus, and many problems exist in its application. However, when fully developed, the electronic torch would be ideal to some type applications such as the spray coating of surfaces with metals vaporized by the high temperature plasma.

The Production of High Temperatures by High Pressure Discharge

It is well known that when a capacitor is discharged, there is a high temperature produced across the spark gap during the discharge. When the inductance of a circuit is reduced to a minimum, the energy released into the gap of an existing capacitor is the maximum energy available in the circuit, and the energy is released with the shortest pulse lengths. In order to use this phenomenon, the "Fischer" capacitor was developed.⁽¹⁷⁾

The Fischer capacitor is a capacitor which surrounds its contained gas coaxially.

Numerous publications have subjected the topic of the actual gas temperature to a rigorous investigation. E. V. Lawrence and F. G. Dunnington, in the Physics Review, Volume 35, 1930, pp. 346., and also J. E. Allen and J. D. Craggs, in the British Journal of Applied Physics, Volume 5, 1954, pp. 446, have contributed articles on this subject.

In these two publications, there was always the related question as to whether or not the time of discharge was long enough to establish within the channel a thermal distribution of the energy according to

Boltzmann. A question which was greatly emphasized was whether or not the electron temperature was in equilibrium with that of the gas molecules.

In this type of high temperature production, the gas surface temperature is determined by the brightness of the spark where by experimental means, it was observed that the spark channel approaches blackbody conditions in the range of 2500-6000 A. (17)

Maximum surface temperatures are produced shortly after the channel achieves opacity, with the pressure and current increasing with the electrical discharge. Beyond this limit, the increase of flux and pressure only increases the maximum current density, widening its pulse, and shifting it behind the current.

Temperatures have been produced in excess of 100,000°K in a pressure of 35 atmospheres in helium. (17) This is very commendable, however, the length of time available for the usage of this high temperature, and its transient production, make this type production of high temperatures inapplicable to most engineering research.

The Production of High Temperatures by Combustion Furnaces

One very conventional means of producing high temperatures is by oxidizing a rich fuel in an insulated container. Such an arrangement can be termed a "combustion furnace". Combustion furnaces have been widely used in industry in the smelting of ores, production of ceramics, production of steam, production of refractory materials and many other processes which require high amounts of heat production at high temperatures.

Combustion furnaces can be constructed to almost any size to operate at, or produce a desired temperature. Extremely large furnaces are used in the production of steam for large power plants.

Combustion furnaces can be designed to operate on almost any type fuel. However, the performance of the furnace will not be as good with a poor fuel as with a rich fuel. In the production of steam for electrical power production, coal, natural gas and oil can be very easily oxidized, producing temperatures in excess of 2000°F, i.e. Unit No. 5, Virginia Polytechnic Institute, operating on crushed coal, has consistently produced recorded temperatures in excess of 2000°F.

Temperatures available in a combustion furnace using a rich fuel are in excess of 2000°C. M. W. Thring⁽³³⁾ states that the theoretical combustion of most rich fuel is approximately 2200°C.

The major disadvantage to the utilization of a combustion furnace, is that in order for a specimen to be heated to the maximum temperature which the furnace is capable of producing, or to any temperature near the maximum temperature of the furnace, the specimen must be placed in the combustion zone of the furnace. This is undesirable since in most investigations, contamination of the specimen is not permissible.

Regardless of this fact, when a specimen is placed in the high temperature combustion zone of a furnace, it will usually be contaminated, desirable or not.

Production of High Temperatures by Electric Furnaces

Electric furnaces capable of producing temperatures greater than 3000°C, in a heating zone of approximately 3 cubic inches have been pro-

duced since 1950.⁽¹⁵⁾ Basically these furnaces have been of the resistance-type furnace utilizing a split-tungsten tube as a heater.⁽¹⁵⁾

In this type furnace an inert atmosphere must be employed in order to achieve maximum temperatures in minimum time. For instance, a test of an inert atmosphere quenching furnace showed that a temperature of 3000°C could be reached in a helium atmosphere in approximately 5 minutes. The same basic furnace, operating with a high vacuum, required approximately 6 hours to reach a temperature of 2600°C.⁽¹⁵⁾ However, it should be noted that in an electric furnace, if an inert atmosphere is desired, the furnace must be evacuated and flooded with the inert gas to be used a number of times whereas the vacuum-type furnace can be evacuated to as high a degree as desired in one operation of the vacuum-pump.

The split-tungsten tube furnace, however, is not the only type resistance furnace. An oxide resistor furnace⁽¹⁸⁾ capable of producing temperatures in excess of 2000°C under oxidizing conditions has been developed by the National Bureau of Standards. However, the difficulties which can be encountered while operating this furnace are usually great enough to prevent this type furnace from being used to any great extent.

Also classified under the category of electric furnaces is the induction furnace.⁽¹⁶⁾ An induction furnace is fundamentally a transformer in which an inductor carrying an alternating current serves as a primary, and the substance to be heated is made the secondary by simply placing it (or a conductive element containing it) in the alternating field of the inductor. The field lines of the inductor are cut by the surface of

the material being heated and induce a flow of energy in the work. The described heating takes place primarily in the surface layers of the heated material. The depth of penetration of the field is dependent upon the frequency of the current used to produce the alternating field - the higher the frequency, the narrower the resultant penetration.

Since the induction coil is not in contact with the work, it can be kept at a low temperature by the circulation of water through a hollow conductor, and the maximum temperature of the work or its conductive container will depend only upon the amount of energy that can be coupled into it and the requirements of protective atmosphere or materials of construction.

Induction heating equipment can be classified according to the means by which the operating frequencies are established, and by the frequencies themselves. Classifications are: electronic circuit, spark gap, rotary converter, mercury arc, and standard a-c power. Spark gap and electronic-circuit-type induction furnaces are the most predominant, however, the rotary converter, mercury-arc, and standard a-c power are the most important in power supply exceeding 30 kilowatts per machine.

Temperatures up to 2500°C have been produced by this type electric furnace. (16)

The Production of High Temperatures by Solar Furnaces

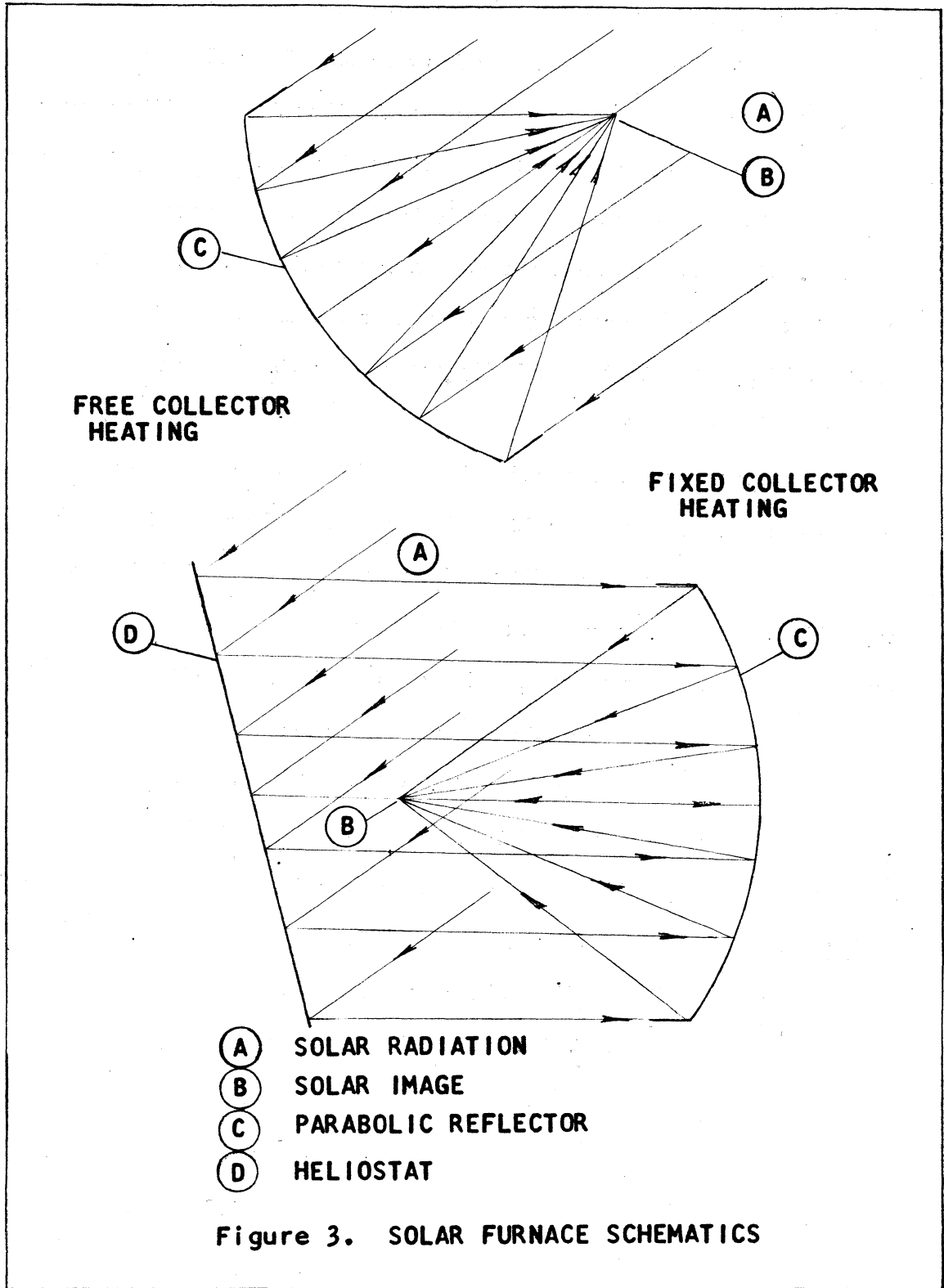
The energy of solar radiation has been known and discussed to a great extent in the past, (7) (24) (3) and almost everyone has witnessed the power of solar radiation when localized by the action of a small convex lens.

Since the rays of solar energy are essentially parallel, if a polished parabolic collector is aligned with the incident solar energy, the rays will reflect radially toward the focus of the reflector. An image of the sun will be formed at the focal plane of the reflector, and the temperature at the focal plane will be proportional to the reflectivity of the collector, and to the size of a collector. Thus it could be said that all the equipment is necessary for a solar furnace is a parabolic collector and some method of aligning the collector with the sun.

Since the position of the sun is constantly changing, if a solar furnace is to be applied for some investigation which requires an appreciable length of time, some method will be required to keep the collector and the sun aligned. The two methods which are used to keep alignment in the application of a solar furnace are: (1) free collector method⁽¹⁹⁾ and (2) fixed collector method.⁽³⁵⁾

In the free collector method, the collector is free to change its azimuth and elevation. The magnitude of the change required to follow the solar path is usually governed by a photocell type control system. In using a free collector solar furnace, one of the prime advantages is that the unit can be completely portable while the limitation of physical size is the disadvantage. See Fig. 3 and Fig. 4.

In the fixed collector method, the collector is made stationary, and the change in solar position is counteracted by a free-swinging heliostat. The heliostat, which is a flat polished reflector, is free to rotate about its vertical and horizontal axes. The advantage of the



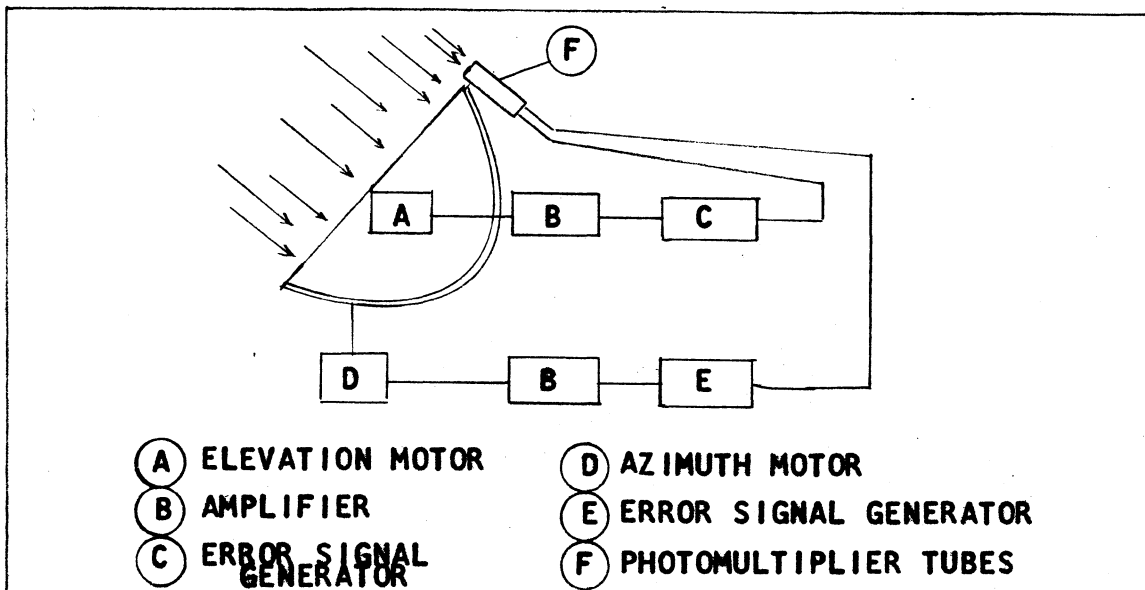


Figure 4. FREE COLLECTOR TRACKING SYSTEM

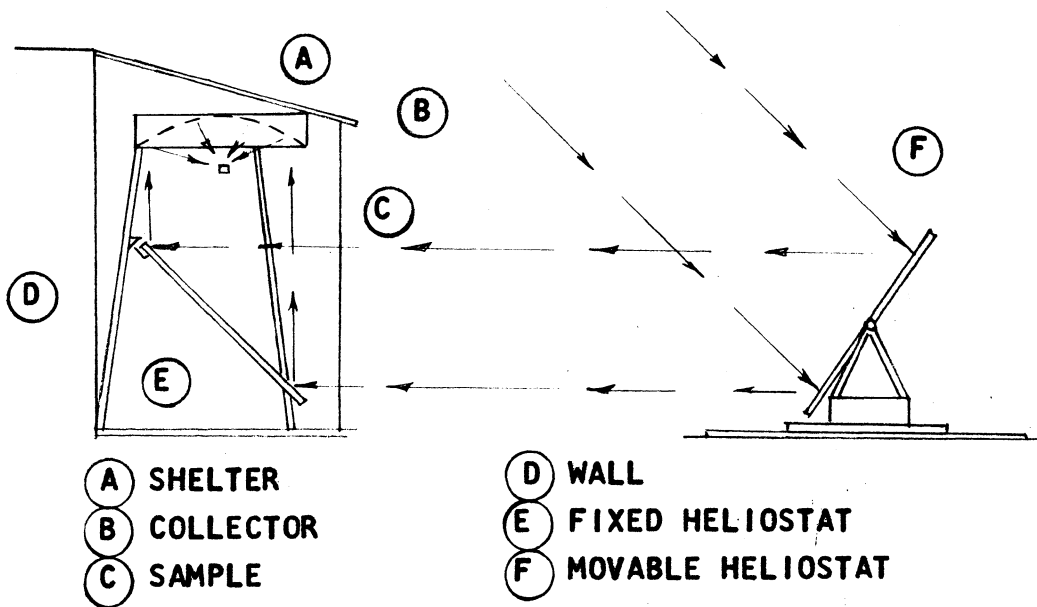


Figure 5. FIXED COLLECTOR INSTALLATION

fixed collector is that it can have much larger physical dimensions than a free collector, while due to its stationary installation, it is not as flexible as a free collector. See Fig. 3 and Fig. 5.

The temperatures produced by a solar furnace are independent of the type of tracking used. Kennecott Copper Corporation has a fixed 60" collector which has produced temperatures of approximately 3000°K, while with the same basic collector, Arthur D. Little, Incorporated,⁽¹⁹⁾ have a free collector capable of 3000°K temperature production. The images produced in these furnaces is of the order of 6 millimeters.

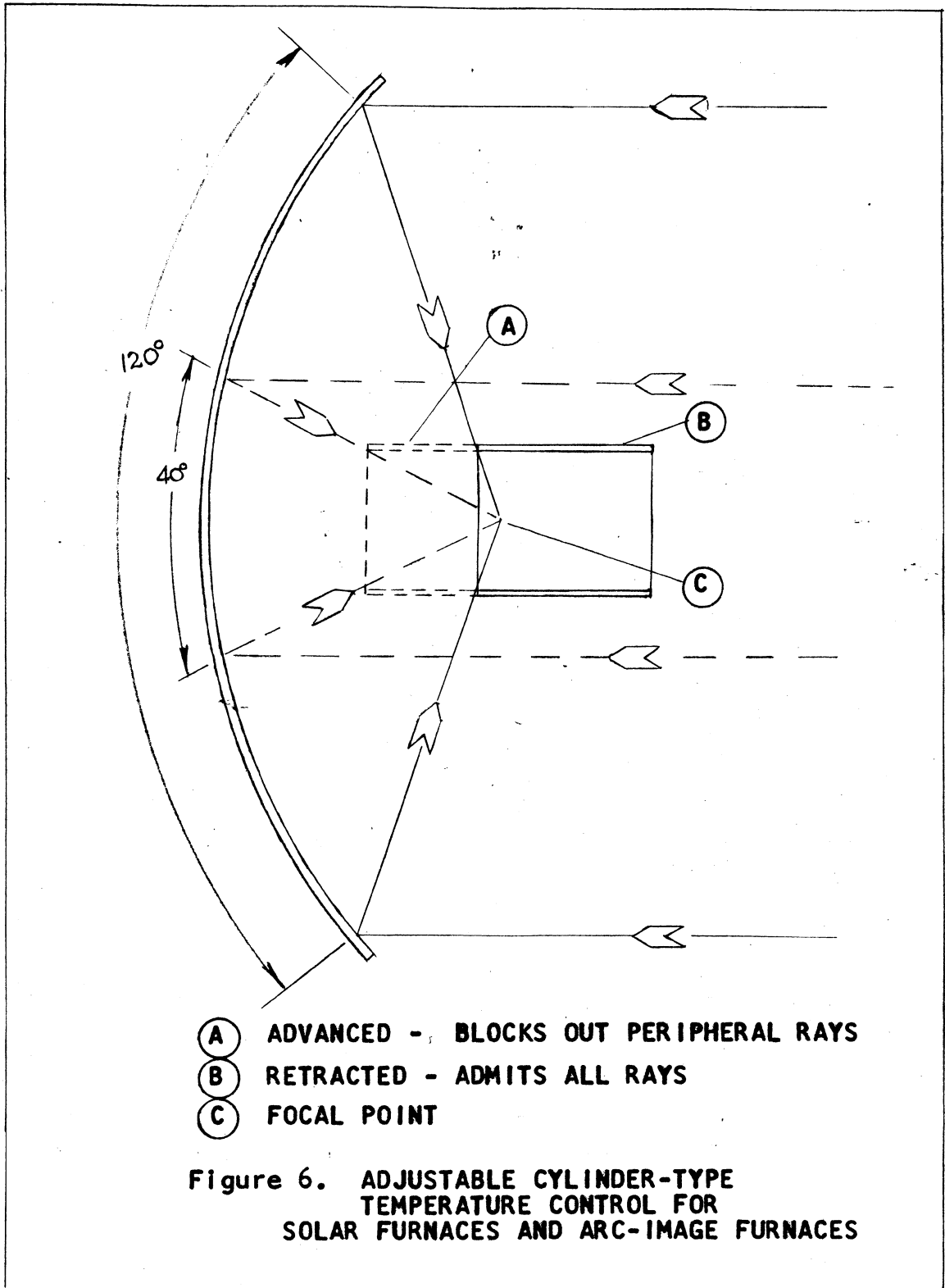
There are several means of temperature control in a solar furnace, one of these methods is shown in Fig. 6.

In 1932, the California Institute of Technology initiated a study of solar energy in conjunction with a solar furnace. This installation is the first solar furnace recorded by the Association for Applied Solar Energy.⁽⁶⁾

The main advantage that a solar furnace exhibits over all but one other type furnaces, is that at the focal plane of the collector, the specimen is heated by pure-radiant energy, which is far enough removed from the source, that contamination of the test sample being heated does not occur. However, the solar furnace is limited in that it can be utilized only during favorable, daylight weather conditions.

The Production of High Temperatures by Direct-Current Arc Furnaces

For many years, the steel industry and many associated industries have utilized the direct-current arc furnace for the production of high temperatures required in many of its processes.⁽²⁹⁾ The temperature



produced in a d-c arc furnace is dependent upon several factors, the major ones being the current passing across the electrodes, the number of electrodes, the configuration of the electrodes, and the atmosphere in which the arc is being formed. Average temperatures of the plasma, which are produced by the current flow across the electrodes, have been developed over 3000°C.

In the basic arc furnace, many conditions exist which cause the apparatus to be inapplicable to many situations which necessitate a high temperature source for investigation. The major condition which would cause the basic arc furnace to be inapplicable in the study of emissivity and emittance is partially the same as encountered in a combustion furnace, this being contamination of surface and surroundings.

There is, however, one type arc furnace which is quite adaptable to the study of emissivity and emittance at elevated temperatures. (28) (30) (9) This type furnace is the arc-image furnace.

The arc-image furnace is similar to the arc furnace in that a high temperature is obtained by the arc formed by the exchange of electrons by the electrodes when activated by a d-c power supply.

Fundamentally, the description of the configuration of an arc-image furnace and its operation is as follows: An arc is formed across the electrodes in a direct-current circuit by the e.m.f. from a direct-current power source. (The temperature of the arc is a function of the current in the circuit and the voltage across the electrodes. In reality, there is a plasma formed in the region of the electron flow and under maximum-ideal conditions the temperature of the plasma is in equilibrium with

the electrons' temperature.)

In the basic arrangement of an arc-image furnace, a parabolic reflector is positioned with respect to the arc such that the arc is at the focal plane of the reflector. Therefore, when the energy, leaving the arc radially, strikes the reflector, it is reflected in parallel beams. Another parabolic reflector of the same size a short distance away, is aligned with the first reflector such that all the energy transferred by the first reflector is gathered by the second reflector and directed toward its focal plane. At the focal plane of the second reflector, an inverted image of the arc produced at the focal plane of the first reflector is formed. This is shown schematically in Fig. 7.

The ideal temperature of the arc-image is a function of the reflectivity of the surface of the mirrors, the deviation from ideal configuration of the reflectors, the absorption of energy by the atmosphere in which the apparatus is located, the dispersion of the parallel light waves as they transverse between the two reflectors, the interference by supports, and the lost energy at or by the arc.

The means of temperature control in an arc-image furnace are the same as those applicable to solar furnaces. See Fig. 5.

This type furnace offers several distinct advantages over the other types of high temperature devices. One major advantage of this type furnace is that it offers a contamination free energy source for the heating of specimens. Another advantage is that the basic components and their arrangement is not so complex as in the electrical type furnaces. In comparing the solar furnace with the arc-image, one finds that the

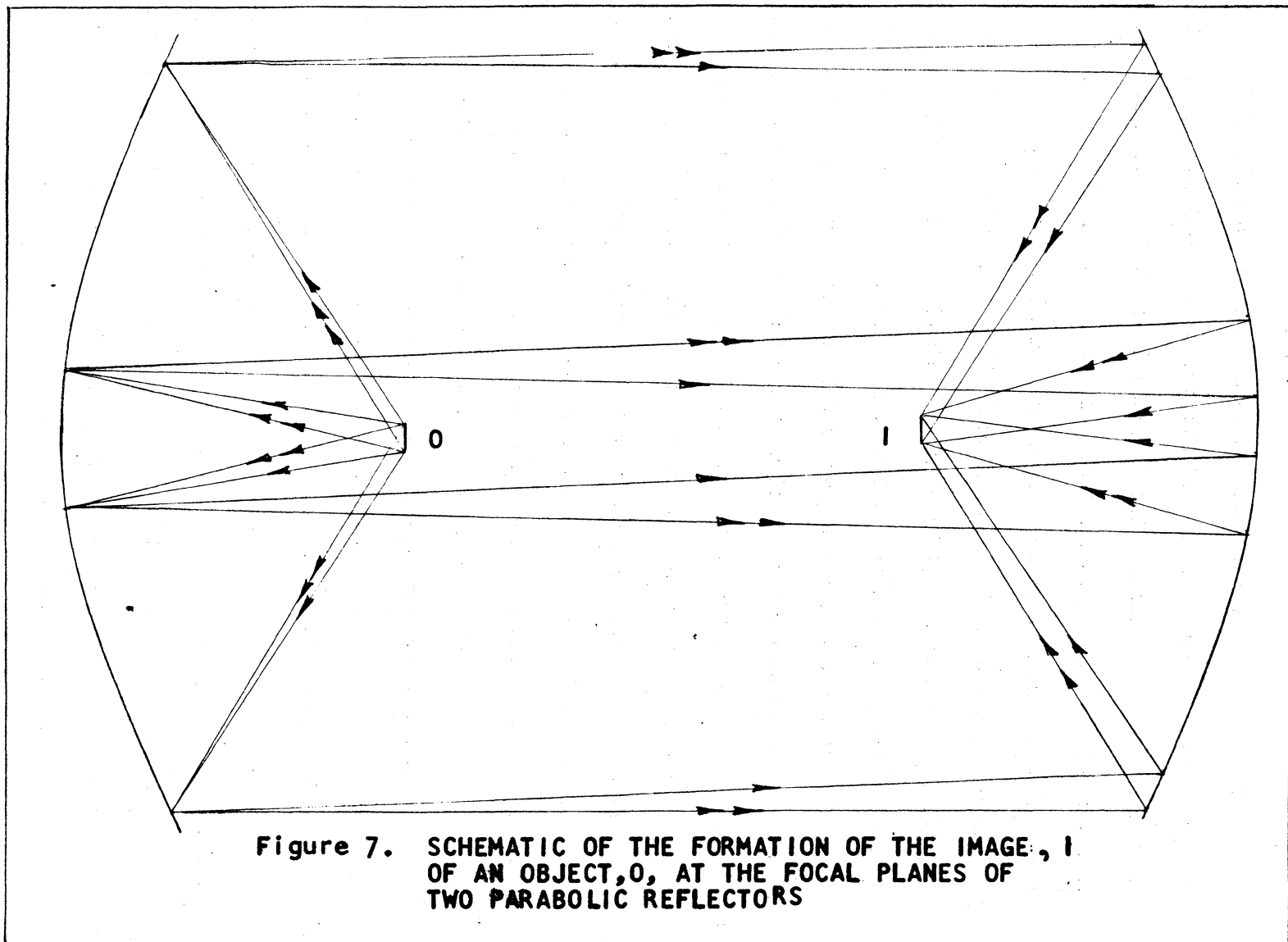


Figure 7. SCHEMATIC OF THE FORMATION OF THE IMAGE, I, OF AN OBJECT, O, AT THE FOCAL PLANES OF TWO PARABOLIC REFLECTORS

solar furnace also has the advantages mentioned above. However, the solar furnace is limited to fair-weather, daylight atmospheric conditions for experimentation whereas a sheltered arc-image furnace can be utilized during any climatic condition, day or night. Also, it must be noted that an arc-image furnace can be designed with much the same physical dimensions of a solar furnace with the same maximum temperature for experimentation. Therefore it has been concluded that the arc-image furnace is the ideal apparatus for the study of emissivity and emittance at elevated temperatures.

To this end, the Mechanical Engineering Department of Virginia Polytechnic Institute, in conjunction with the Ceramic Engineering Department of Virginia Polytechnic Institute, has procured two 60" General Electric search lights.

Since this equipment will be concerned with emissivity and emittance at elevated temperatures, it follows that a discussion of the previous techniques utilized in the evaluation of emissivities and emittances at low and high temperatures and the methods by which elevated temperatures can be determined will be of value to future investigators.

Previous Methods of Determining the Emissivity or Emittance of a Surface

In studying emissivity and emittance at elevated temperatures, a discussion of previous techniques used to determine this property is warranted. The methods of determining the emissivity or emittance to be discussed are: Hutchins' Method, Royd's Method, Nutting's Method, Wilkes' Method, Schmidt's Method, Dobbins' Method, Dunkle and Gier's Method, Aref's Method and Metzger's Method.

(It is realized that these methods do not represent all the research which has been done on this subject. However, these methods represent, to the authors knowledge and research, the earliest and/or most successful methods of investigation.)

Hutchins' Method

In 1898, Hutchins⁽²²⁾ utilized a method of determining the reflectivity of a sample surface to determine the emissivity of the surface. Basically, this method consists of placing a sample in a region of known or determinable incident solar radiation and measuring at 10° stations from the normal to the surface, the energy which is reflected from the specimen.

By assuming the Cosine law holds, and assuming that the energy at each 10° station corresponded to the first assumption, a curve for reflectivity versus reflectance angle could be plotted.

Since the specimen is in a region of previously determined incident energy, the reflectivity of the surface can be determined. In opaque

bodies, the emissivity of a surface is equal to unity minus the reflectivity.

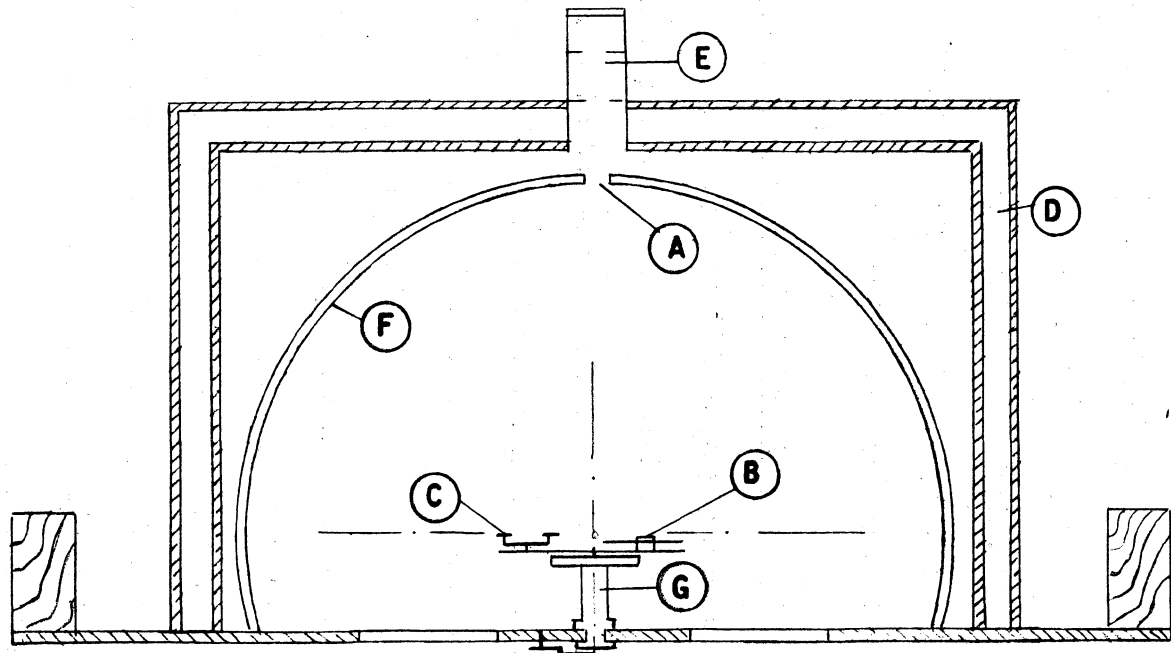
Therefore Hutchins' method, which neglects the direct energy emitted by the specimen, can be considered an indirect method of determining the emissivity of a surface. Obviously, this method is inherently inaccurate, however, it is also inherently simple. Thus, this method would be limited to applications which require simplicity rather than high accuracy, and to applications where the temperature of the specimen is below 700°R.

Royd's Method and Coblentz's Method

In 1911, Royd's published a paper concerning the determination of reflectivity by means of an absolute integrating radiometer. At that time, W. W. Coblentz⁽⁵⁾, was well along with investigation utilizing the same type apparatus. Since that time, H. E. Beckett in 1931, and R. C. Birkebak⁽³⁾, in 1956, have utilized the same basic method and apparatus in further investigation.

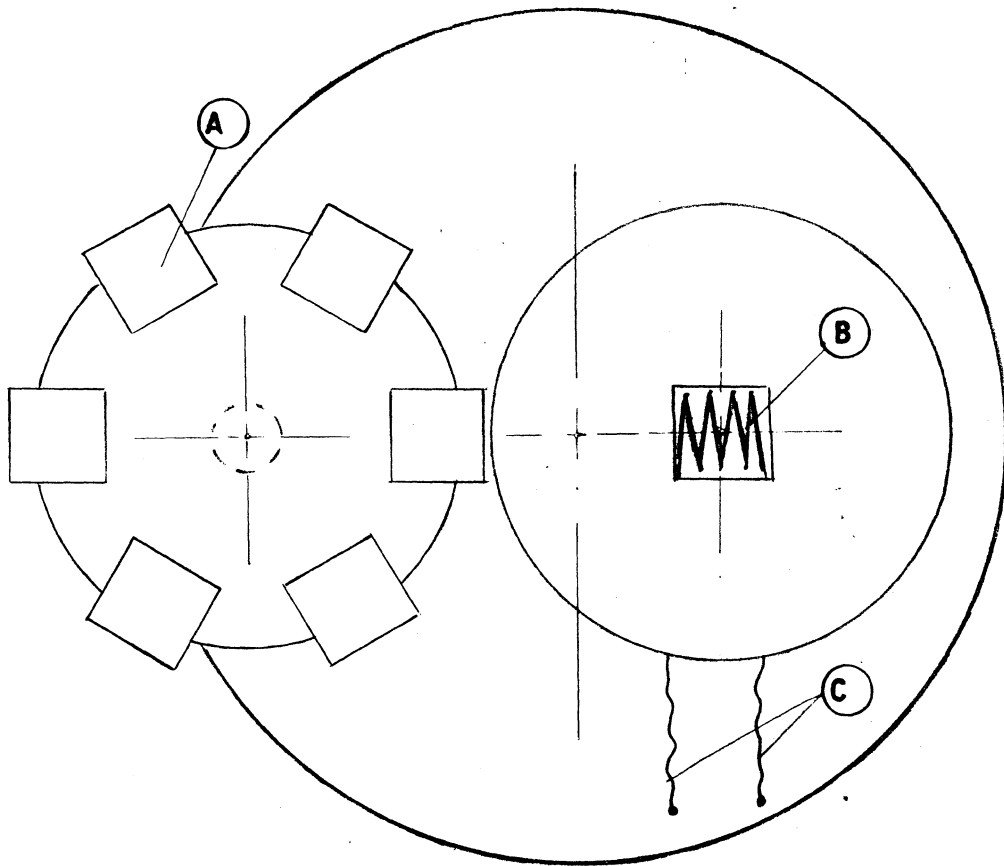
This method incorporates a hemispherical reflector as the major component, and a thermopile. Through the aperture at the center of the hemisphere, radiation from a source, usually the sun, is brought into contact with a sample located along the base diameter of the hemisphere. Located equidistantly from the center of the base diameter, and on the base diameter, is the thermopile, such that all of the entering energy which is reflected by the specimen, will be collected or integrated by the thermopile. This arrangement, as shown in Fig. 8 and Fig. 9, places the test specimen and the thermopile at conjugate foci of the hemisphere.

After measuring the reflectant energy from the test specimen with



- | | | | |
|-----|---------------------|-----|---------------------------------|
| (A) | APERTURE | (E) | SIGHTING TUBE AND QUARTZ WINDOW |
| (B) | THERMOPILE | (F) | POLISHED ALUMINUM SURFACE |
| (C) | TEST SURFACES | (G) | ADJUSTABLE AND ROTATABLE STAND |
| (D) | WATER-COOLED JACKET | | |

Figure 8. ABSOLUTE INTEGRATING RADIOMETER



- (A) TEST SURFACES**
- (B) THERMOPILE RECEIVING SURFACE**
- (C) THERMOPILE LEADS**

Figure 9. TOP VIEW OF THERMOPILE AND TEST SURFACE ADJUSTABLE STAND

the thermopile, the thermopile is repositioned such that the entering energy falls directly upon it, thereby giving an indication of the energy which fell upon the test specimen.

By taking the ratio of the total energy falling upon the test specimen and the energy reflected as determined by the thermopile, the reflectivity of the sample's surface is determined. It is necessary to apply correction factors to account for the energy which is absorbed by the hemisphere, and the energy which escapes through the aperture. This can be done with a reference surface in conjunction with the thermopile.

This method is limited by the amount of solar radiation which is available to heat the specimens. Therefore, the temperature limit for study is approximately 600°R.

Nutting's Method

In 1912, P. G. Nutting developed another indirect method of determining the emissivity of a surface.

This method utilizes a device for measuring reflected energy in the visible region of the spectrum and comparing the relative brightness of the surface to that of a diffuse illuminator. Neglecting multi-reflections and directly emittant energy, the reflectivity of the surface becomes the ratio of the brightness of the test surface to that of the diffuse illuminator.

Wilkes' Method

G. B. Wilkes⁽³⁴⁾ developed a method of determining the emissivity of a test sample by comparison with two reference samples, one coated

with magnesium ($\alpha = 0.15$) and the other coated with lampblack ($\alpha = 0.97$). The amount of incident energy, usually solar, is measured with an Epperly pyrhelimeter.

In this method, samples and reference surfaces are suspended four inches in diameter. The elevation of the specimens is to eliminate conduction losses, also to minimize losses by radiation, the underside of each specimen is covered with aluminum foil.

When the specimen temperatures reach equilibrium, they are measured concurrently with air temperatures and pyrhelimeter readings. Using these values, the emissivity or absorptivity of the surface can be calculated using the following equation:

$$J_i \alpha_s = \epsilon \sigma (T_2^4 - T^4) + h \Delta t_s \dots\dots\dots (1)$$

Since $\alpha = \epsilon$, equation (1) reduces to:

$$\epsilon = \frac{h \Delta t_s}{J_i - \sigma (T_2^4 - T^4)}$$

Where:

T = effective "sky" temperature determined by two reference samples

T₂ = surface temperature

h = coefficient of convection determined by two reference samples - $\frac{\text{Btu}}{\text{hr-ft}^2\text{-}^\circ\text{F}}$

J_i = incident energy - $\frac{\text{Btu}}{\text{hr-ft}^2}$

Δt_s = temperature difference

σ = Stefan-Boltzmann constant

ε = emissivity.

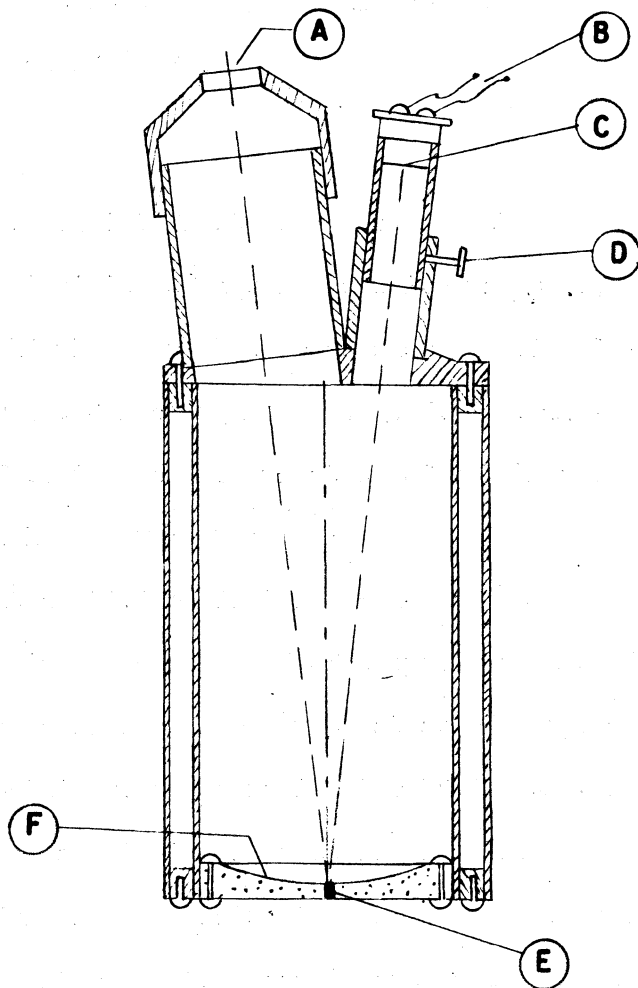
Wilkes' method has limitations similar to those confronted in Royd's method, in that the simple solar radiation will not produce temperatures in excess of 600°R.

Schmidt's Method

In 1930, E. Schmidt first described a method^{(13) (23) (4)} for determining the emissivity of a surface which makes use of radiometer containing a gold plated reflector as shown in Fig. 10. This method has been used quite effectively by E. R. G. Eckert, J. P. Hartnett and T. F. Irvine, Jr., in the determination of total emissivities of porous materials below 1100°K^{(13) (23) (24)}.

The apparatus utilized in this method of study basically consists of: an ideal radiator constructed of copper, painted black and heated electrically, a galsa wood frame with attached copper heating plate, a water cooled container, and a radiometer having a gold plated reflector and a thermopile, and is illustrated in Fig. 11.

The procedure for utilizing this apparatus is as follows: The ideal or blackbody radiator and test sample are heated by electrical power to the desired temperature, and the temperature surrounding the test specimen is maintained constant by controlling the flow of water through the container. The radiometer is sighted into the blackbody radiator, then onto the test specimen, and then into a "blackbody" cavity in the container. Readings of the reflections of a galvanometer hooked to the thermopile in the radiometer are recorded for each sighting. Temperatures of the blackbody radiator, test sample, and blackbody cavity are determined by the use of thermocouples.



- | | |
|----------------------------------|-------------------------|
| (A) APERTURE | (D) SET SCREW |
| (B) THERMOPILE LEADS | (E) SIGHTING HOLE |
| (C) THERMOPILE RECEIVING SURFACE | (F) GOLD SURFACE MIRROR |

Figure 10. RADIOMETER

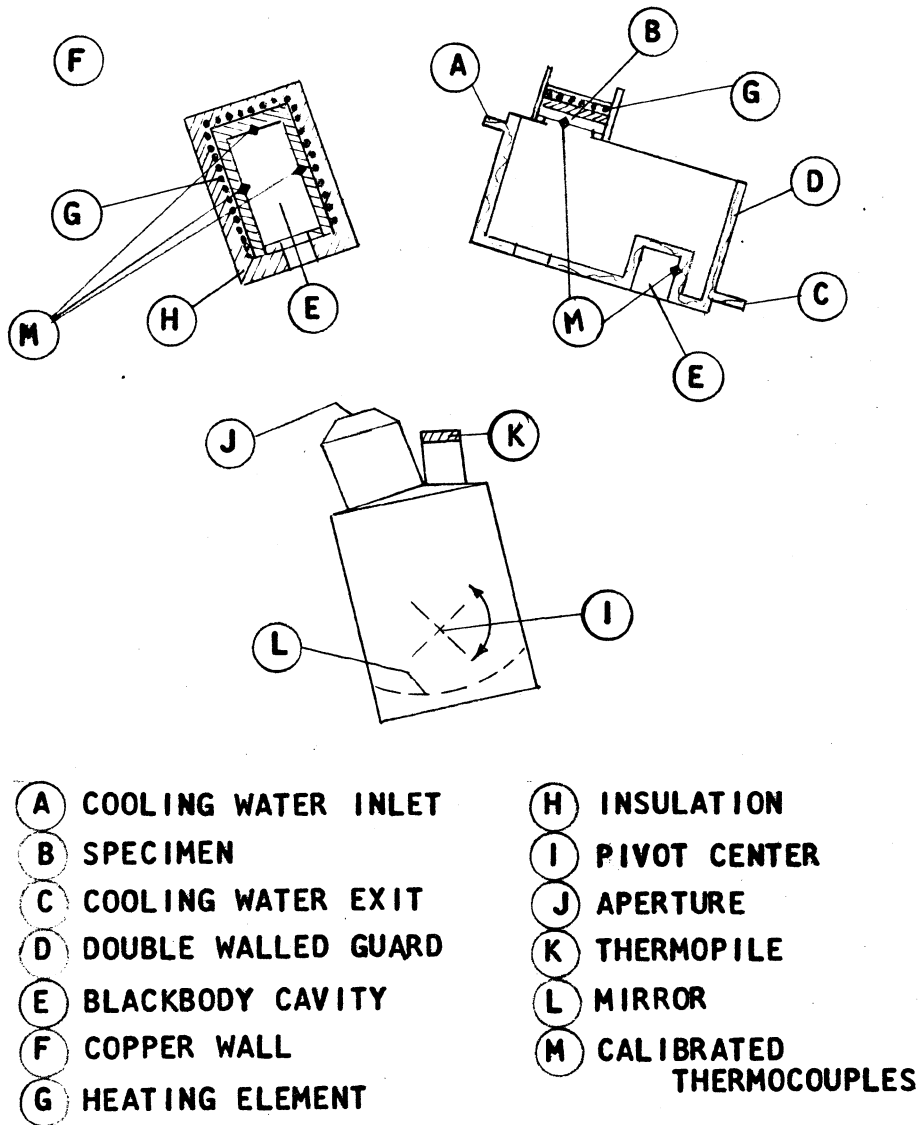


Figure 11. SCHEMATIC OF APPARATUS FOR THE DETERMINATION OF EMISSIVITIES

The emissivity of the surface can then be calculated by the following equation:

$$\epsilon_s = \frac{(T_b^4 - T_g^4) (\Delta_2 - \Delta_3)}{(T_s^4 - T_g^4) (\Delta_1 - \Delta_3)} \dots\dots\dots (2)$$

Where:

T_b = temperature of ideal radiator

T_g = temperature of cavity

T_s = temperature of surface

Δ_1 = galvanometer deflection of radiometer sighted at ideal radiator

Δ_2 = galvanometer deflection of radiometer sighted at test surface

Δ_3 = galvanometer deflection of radiometer sighted at cavity.

The limitations of this type apparatus are basically in the determination of the temperature of the specimen. Thermocouples can be used quite accurately at temperatures approaching 2000°K, however, the fidelity and physical characteristics of most thermocouples begin to undergo changes at temperatures in excess 2000°K.

Dobbin's Method

During the annual meeting of the American Society of Mechanical Engineers in 1950, John P. Dobbins presented a paper which described a method by which the emittance of an oxidized surface can be calculated. The following description of this method is taken from Dobbin's paper "Emittance of Oxidized Metals". (11)

"Calculations for Simple Materials. The emittances of ideal-

ized polished opaque bodies, i.e. the emissivities of the materials of which specimens are composed, can be computed quite closely in most cases from other known properties of the subject materials by established theoretical methods. To illustrate, the emissivities of metals, ϵ_m , may be evaluated from their corresponding electrical conductivities, $K \left(\frac{\text{mho}}{\text{cm}} \right)$

at the same temperature. Spectral values at any wave length λ (cm) are given by the Hagens-Rubens relationship -

$$\epsilon_m = 0.365 (K\lambda)^{-1/2} - 0.067 (K\lambda) \dots\dots\dots (a)$$

"Integral emissivities at temperatures T(°K) are correspondingly given by the Aschkinass-Foote relationship -

$$\epsilon_m = 0.575 (T/K)^{1/2} - 0.178 (T/K) \dots\dots\dots (b)$$

"The theoretical results obtained by this equation are recognized generally to be in "very satisfactory agreement with experiment". It should be noted however that at high temperatures (where appreciable fractions of radiant energy are in the short-wave spectral region) the correlation between predicted and observed values may be less satisfactory in some cases.

"Similarly for most non-metals, the spectral emissivity can be evaluated from measured reflectivities, $r = 1 - \epsilon_\lambda$, or from known refractive indices, n, by means of Fresnel's well known formula for normal incidence:

$$r = \left(\frac{n - 1}{n + 1} \right)^2 \dots\dots\dots (c)$$

"Variation of refractive index with wave length, over the spectral region corresponding to thermal radiations, must be small in order to use equation (c) for total reflectivities without the complication of having to perform integrations over each of the regions considered, to obtain representative average values for total radiation. For most materials, on the basis of incomplete data, this appears fortunately to be the actual situation. Contrary to the usually valid generalization of Hottel that "the emissivities of nearly all substances increases with temperature", however, the indications are that for most non-metals at temperatures appreciably above 500°K (ca. 500°F) the reverse situation holds; as their refractive indices in general tend to decrease with increasing wave length (decreasing radiation temperature) in the significant regions of the thermal radiation spectrum where this property has been measured. A usually small decrease in refractive index at a given wave length which occurs with increase in temperature, due to density change, partly masks the above effect.

"Calculations for Complex Specimens. Depending upon the thickness of oxide film present on a sheet of metal, the emittance of the sheet will vary from a minimum value, corresponding to that of a pure polished metal, to a maximum value, corresponding to that of the rough oxide. Between these extremes lie intermediate emittances, the values of which can be calculated

for various specified conditions of oxidation. For example, if it be assumed that the oxide is very thick and has a smooth surface, then the emittance for the sheet corresponds to the emissivity of the oxide. Thick oxidized surfaces which are rough may exhibit emittances even greater than the emissivity of the oxide. For thin films, by contrast, temper colors (due to invisible interference phenomena) will appear, and the emittances are found to lie intermediate between those for the bare metal and those calculated for moderately thin films. As the oxide film initially forms and then increases in thickness, first the ultra-violet short wave lengths are poorly reflected, later the visible light, and lastly the long infa-red. When passing through the visible region, the color sequence observed is amber, magenta, purple, blue, gray; corresponding to the destruction by interference of the complementary wave lengths. Bluish oxides, for example, result from the subtraction of the long waves of the visible spectrum, i.e. from the elimination of the reds, yellows, and oranges from the incident white light. These wave lengths must be a whole-integer multiple of twice the film thickness for such interference to occur. For oxide films of intermediate thickness, the emittances may be computed from the resultant of internal reflectivities, as follows:

- (1) The reflectivity of the oxide, r_{OX} , and its emissivity $\epsilon_{OX} = 1 - r_{OX}$ are computed from the known refractive index in air, by eq. (c).

(2) The reflectivity of the metal, r_m , relative to the air (or more strictly to a vacuum) is computed from its known electrical conductivity by equation (a) or (b) (depending upon whether spectral or integral values are desired), together with the defining relationship, $r_m = 1 - \epsilon_m$.

(3) The refractive index of the metal, n_m , in air is computed from the approximate expression for normal reflectivity

$$r_m = 1 - \frac{2}{n_m}; 1 - r_m = \frac{2}{n_m} - \epsilon_m \dots\dots\dots (d)$$

Further discussion of the origin and accuracy of this equation is given later.

(4) The corresponding index of the metal relative to its oxide, n_m^i , is then found from the usual relationship for change of refractive index with boundary material

$$n_m^i = \frac{n_m}{n_{ox}} \dots\dots\dots (e)$$

(5) By substituting this new reduced refractive index, n_m^i , back into equation (d), the approximate normal emissivity of the metal relative to its oxide is found as

$$\epsilon_m^i = n_{ox} \cdot \epsilon_m \dots\dots\dots (f)$$

(6) The emittance ϵ (large script) of the composite metal-oxide double layer (which, according to Kirchoff's Law, is equal to its absorptance, A ,

for radiation from a blackbody at the same temperature) may then be found by an equation which into both the external and sum of all internal reflections, namely

$$\epsilon = (\epsilon_{\text{ox}}^{-1} + \epsilon_{\text{m}}^{-1} - 1)^{-1} \dots\dots\dots (g)$$

... This equation ... is valid for metals coated with relatively smooth layers of non-opaque oxides ..."

Dobbin's method has been shown quite valid in applications below 1000°K by experimental comparison. Above this temperature, there is significant deviation between analytical and experimental values.

Dunkle and Gier's Method

In September of 1950, R. V. Dunkle and J. T. Gier⁽¹²⁾ published a paper in which they described another method by which the absorptivity of a surface could be determined.

The Dunkle and Gier method is a comparative type method which fundamentally consists of placing a test sample and a reference sample in incident solar radiation, and placing an identical test sample and reference sample in similar, tubular but shielded containers. After the exposed test sample and reference sample have reached equilibrium conditions, the shielded test sample and reference sample are heated by electrical energy until they reach the same temperature as the exposed samples.

Since the incident solar energy is equal to the amount of electrical energy required to raise the shielded reference sample divided by the surface absorptivity and area, similarly, the energy absorbed by the test

sample is equal to the heat input required to raise the temperature of the shielded sample up to the temperature of the exposed test sample.

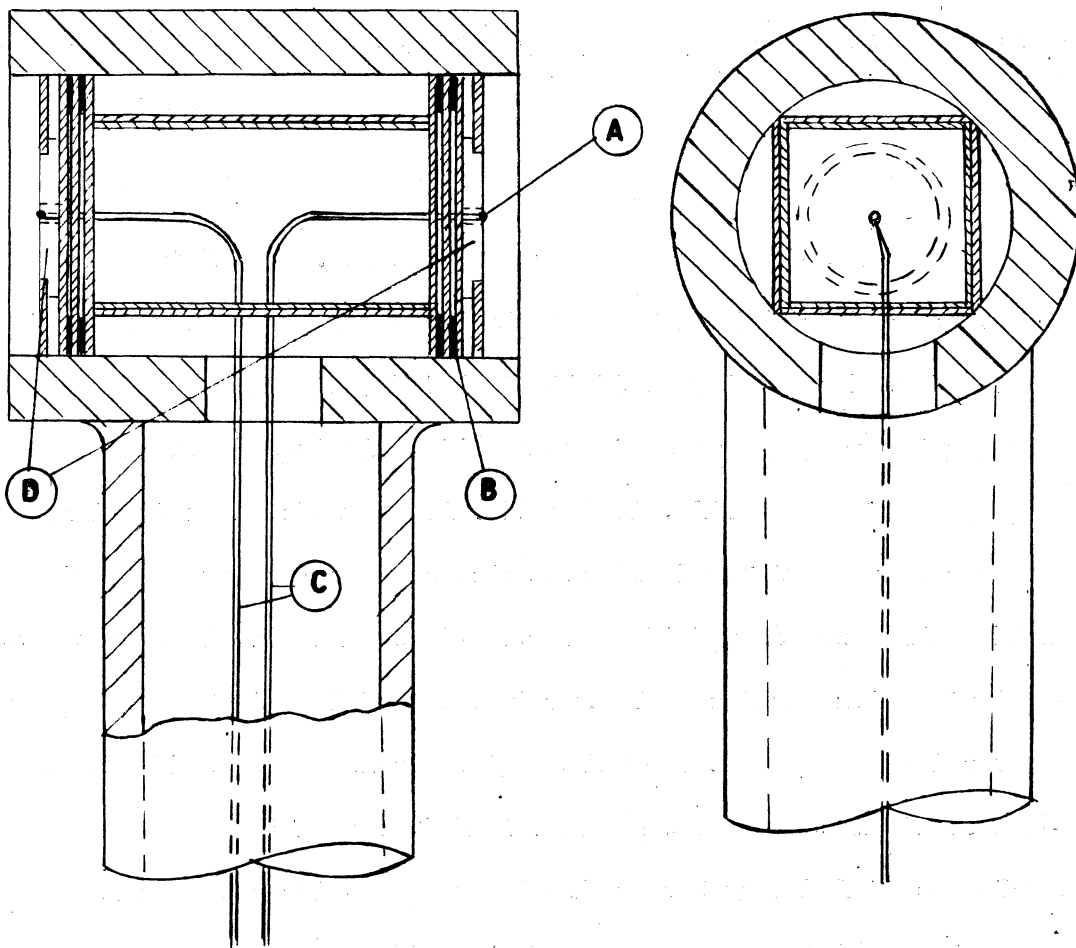
The absorptivity of the test sample can then be determined by using the ratio of the two heat inputs and the known absorptivity of the reference sample.

Aref's Method

In August 1958, M. N. Aref⁽¹⁾ described a direct-comparative method for the determination of the emissivities of industrial surfaces. This method makes use of an insulated air-tight container, silica tube, refractory plugs, electrical heating element, thermocouples and probe-type radiometer, as shown in Fig. 12 and Fig. 13.

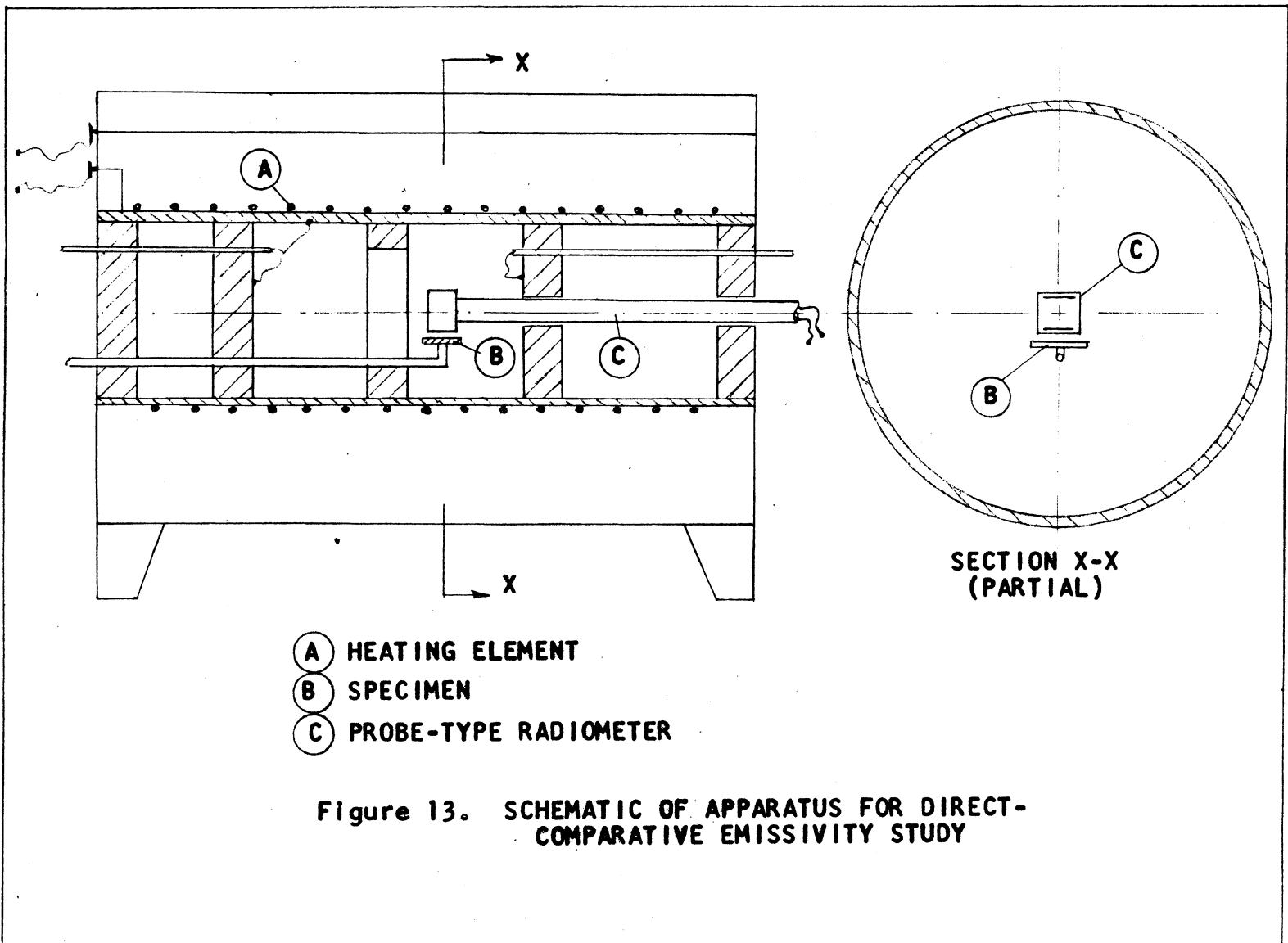
A probe-type radiometer consists basically of two insulated-steel heat exchange disks held back to back in a high heat resisting silica body by means of mica disks and washers. If this type radiometer is placed in a blackbody enclosure, there is no response by the instrument since there is no differential heat flux on the two steel disks. However, when a test specimen is brought close and parallel to one of the disks, a response will be obtained from the instrument to represent the heat flow which results due to the difference in the emissivity of the specimen and the blackbody enclosure.

The procedure for the use of this apparatus is as follows: first, the blackbody heat enclosure consisting of the silica tube, refractory plugs and heating element is brought up to temperature. The probe-tube radiometer and test specimen are then inserted into the blackbody cavity such that the radiometer is not effected by the test specimen. The heat



- (A) THERMOCOUPLE JUNCTION
- (B) MICA DISCS AND SPACERS
- (C) THERMOCOUPLE LEADS
- (D) STEEL DISCS

Figure 12. CROSS SECTION OF PROBE-TYPE RADIOMETER



flux from the blackbody enclosure is then determined by the radiometer. Next, the test specimen which is at the same temperature as blackbody enclosure is positioned beneath the probe type radiometer.

If the emissivity of the test specimen is less than unity, the differential heat flux, Q_R , will be indicated such that by use of calibration curves for the potentiometer, the heat flux from the test specimen can be determined. Then if the heat flux from the blackbody enclosure, Q_B , is determined for the temperature of the blackbody enclosure, the emissivity, ϵ , of the specimen can be determined by the relation:

$$Q_B - Q_e = \epsilon \cdot Q_B$$

or

$$\epsilon = 1 - \frac{Q_e}{Q_B}$$

Since Aref's method utilizes conventional thermocouples, its application is limited to temperatures below about 2000°C.

Metzger's Method

In June 1959, J. W. Metzger⁽²⁸⁾ presented a thesis at Drexel Institute of Technology which described a method by which the spectral emissivities of surfaces can be determined. Metzger's work presents what is probably the first research in the field of high temperature emissivity with an arc-image furnace.

Metzger's method basically consists of energizing a test specimen at the focal plane of a 60" General Electric searchlight reflector. The apparent temperature of the surface is determined with a calibrated optical pyrometer. After observation by the optical pyrometer, the spectrum being

produced by the test specimen, is automatically scanned and recorded by a spectrometer.

The data obtained with the optical pyrometer and the spectrometer can be reduced by the application Wein's Law, and Planck's Law.

In order to utilize Planck's Law in the analysis of the data recorded by the true temperature of the specimen is required. Wein's Law for use with optical pyrometer reduces to:

$$\frac{1}{T_A} - \frac{1}{T} = \frac{\lambda}{C_2} \ln \epsilon$$

where:

T_A = true temperature (actual)

T = apparent temperature

λ = wave length, microns

ϵ = emissivity at T_A ,

A true temperature is assumed, and from available literature a spectral emissivity at the wave length of the optical pyrometer ($\lambda = 0.65\mu$) is obtained. The apparent temperature is then employed with the assumed true temperature to calculate the spectral emissivity. If the calculated spectral emissivity does not agree with the spectral emissivity corresponding to the assumed, further assumptions are made until values of spectral emissivity agree.

Having the true temperature of the sample's surface, the spectral emissivities of the specimen can be determined from Planck's Law:

$$\epsilon_{\lambda T} = \frac{W_{\lambda T} [e^{(C_2/\lambda T)} - 1]}{C_1 \lambda^{-5}}$$

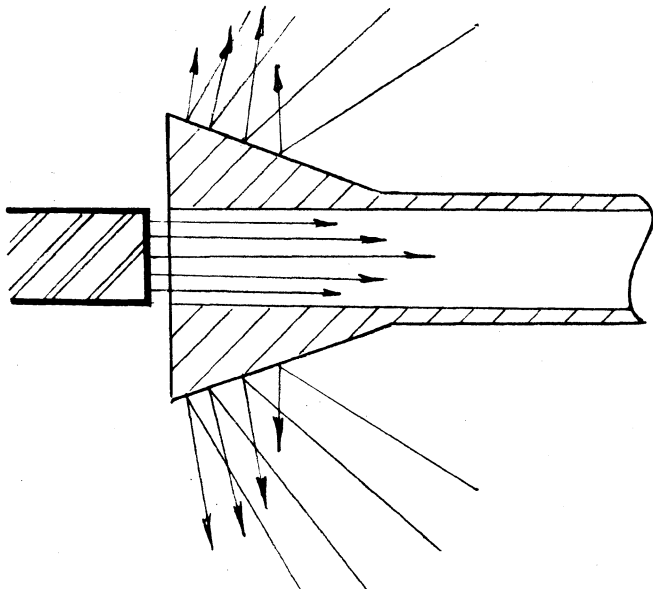
When using optical pyrometers or total radiation pyrometers in the study of surfaces with emissivities less than unity, there must be some

means of selecting or metering only the emitted radiation due to the fact that the energy reflected by the surface will cause errors in the pyrometer readings.

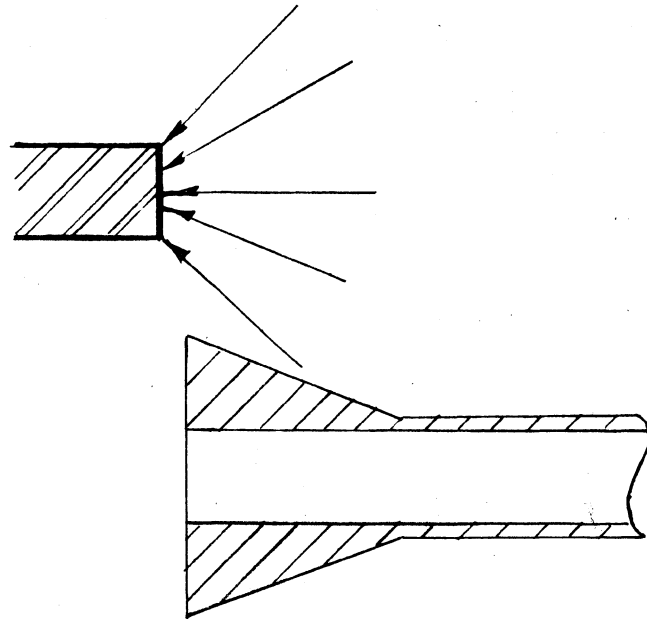
In order to eliminate errors arising from surface reflectivity in optical pyrometer observations of test surfaces, Metzger incorporated a mechanical discriminator which was first basically described by W. M. Conn and G. Braught in the January, 1954, issue of The Journal of the Optical Society of America. The operation of the discriminator is illustrated in Fig. 14.

Metzger's mechanical discriminator consists of four funnel-tubes and an annular baffle ring which is driven by a 1750 revolutions per minute, 1/6 horsepower, 220 volt A.C. motor, through a one to one gear train. When the funnel tubes are not directly facing the test surface, the surface is being heated by the radiation from carbon-arc, and the energy re-radiated, is wasted. However, when the funnel tube completely faces the specimen, no energy can strike the test surface, so that a radiation pyrometer reading at that instant has no error introduced due to the reflectivity of the test surface. When the discriminator is in the heating position, the annular baffle ring intercepts the energy which would fall into the pyrometer, so that the pyrometer readings are due to radiated energy alone. Since the pyrometer views the object only a small portion of the time, it is necessary to calibrate the pyrometer in conjunction with the discriminator and some known temperature sources.

Metzger was not completely satisfied with the results of the work which he performed. This was due to the fact that his investigation was directed at the emissivity of a surface (or, the emittance of a pure



**FUNNEL BLOCKS SOURCE RADIATION
FROM SPECIMEN - TRANSMITS
SPECIMEN RADIATION TO DETECTORS**



**HEATING PORTION OF CYCLE -
SOURCE RADIATION REACHES SPECIMEN
RERADIATED ENERGY IS WASTED**

**Figure 14. OPERATION OF MECHANICAL
DISCRIMINATOR**

surface) and at the temperatures of his investigation (1100 - 1800°K) the oxygen content in an inert atmosphere of argon quickly contaminated the surface of a test sample even though the inert gas had been passed through a passage packed with granules of titanium to absorb any oxygen in the argon.

The limitation of this method lies in the determination of the actual temperature of the specimen. At the present time, little information is known of the spectral emissivities of substances at 0.65μ at more elevated temperatures.

Incandescent Temperature Measurement

In the study of the characteristics of materials at incandescent temperatures, i.e., temperatures above about 1000°F (540°C), the determination of the true temperature of the test sample is usually of prime importance. Emissivity and emittance studies require very high accuracy in the determination of temperature, due to the fact that when calculating the emissivity or emittance of a surface from the Stefan-Boltzmann Law, the emissivity is inversely proportional to the fourth power of the absolute temperature of the surface radiating energy.

When measurement of temperature in excess of 1000°F, there are only three types of devices of accurately determining temperatures of specimens under study. These devices are thermocouples, radiation pyrometers and calorimeters. Discussion of these devices follows immediately.

Thermocouples

Since the time of their first application, thermocouples have advanced steadily toward higher temperature applications. Base metal thermocouples can satisfactorily measure temperatures approaching 1300°C, platinum-platinum-rhodium thermocouples can be used at temperatures approaching 1900°C, and iridium-iridium-ruthenium thermocouples are quite applicable to temperatures as high as 2300°C⁽³¹⁾.

The iridium-iridium-ruthenium thermocouple was first introduced in 1933 by O. Fuessner, a German scientist, who reported that the thermocouple has a nearly linear e.m.f. temperature relation, and measures 10.85 mv output at 2000°C. This sensor opened the gateway to temperature

measurements up to 2000°C. The National Bureau of Standards recalibrated this thermocouple for the measurements of temperatures in the after-burners of jet engines.

Between 1948 and 1950, The Armour Research Foundation conducted investigation toward the development of thermocouples, alloy wire and refractory metals of ruthenium, rhenium, osmium, tantalum, niobium, molybdenum, iridium and rhodium.

G. Steven⁽³²⁾ reported in High-Temperature Technology, "The combination of iridium and iridium-rhodium alloys fulfilled the requirement of a metallic thermocouple which can operate, unprotected in the temperature range of 1600°C to 2000°C when ambient atmosphere contains oxygen.

"In the temperature region between 1000°C and 2100°C, the most desirable properties are shown by the tungsten-iridium thermocouple. The thermoelectric characteristic curve is almost straight; the e.m.f. output is highest and, in helium, remains constant for 120 hours at 2000°C. The e.m.f. gradient is twice that of platinum-platinum - 13% rhodium. The use of pure metals eliminates calibration difficulties associated with compositional difference of alloy wires. Finally, compensating leads are not usually required because of the low e.m.f. output up to 100°F."

Thermocouples have also been developed which are metal-ceramic and completely ceramic in character. It has long been the goal of refractory technologists to develop an extremely high temperature thermocouple of two oxidation-resistant refractory materials. At this time, only three non-metallic materials have found acceptance as high temperature thermocouples, namely, graphite, silicon carbide and boron-carbide.

G. Steven further reported in High-Temperature Technology, "The graphite-silicon carbide thermocouple developed by G. R. Fitterer has been used to measure the temperature of molten iron and steel. One element of this thermocouple is a silicon carbide rod set coaxially in a closed-end graphite tube which forms the other leg of the thermocouple. To form a cold junction, the upper ends of the element are generally water cooled. The electromotive force of this thermocouple is one magnitude greater than that of metallic 'couples. At 1650°C (3000°F) this temperature sensor is reported to generate almost 0.5 volt."

"A tungsten-graphite thermocouple was described by H. L. Watson and H. Adams in 1928, and at least one reference has been noted in Russian literature. F. Holtby used a smaller assembly in order to reduce the heat capacity and make the sensor suitable for use in small crucibles. The earlier form of this device utilized a tungsten rod under compression supplied by a hollow graphite tube and a water-cooled junction end. The graphite element was a 5/16-inch spectrographic electrode that was "annealed" between 1800°C and 2000°C before use. The advantages claimed for this thermocouple are: (1) a reasonably high e.m.f., about 38 mv at 1650°C; (2) good sensitivity, about 1.25 mv/100°F at 1650°C (3000°F); (3) relatively simple design; and (4) negative cold-junction compensation. In later models, separate tungsten and graphite elements were used, and the electric circuit was closed by the molten metal in the bath."

"R. R. Ridgway investigated the properties of the graphite-boron carbide thermocouple. The patent claim includes a calibration to 2500°C (4530°F) with an e.m.f. output of 0.7 volt at that temperature. It is further claimed that the thermocouple is stable during long periods of

high temperature exposure."

"H. T. Clark compared the tungsten-graphite with the graphite-silicon carbide thermocouple and summerized their advantages and disadvantages. Both thermocouples were used to about 1800°C (3270°F) and were not impaired by rapid temperature changes. When taking immersion temperature measurements in a molten metal bath, the graphite crucible had to be protected from attack by the liquid slag."

Due to many factors, i.e., the absorption of moisture, non-metallic thermocouples are not suited for extremely accurate research at high temperatures. For usage in arc-image furnaces, the non-metallic thermocouples are too large for convenient positioning. Further, non-metallic thermocouples, even though they can be used at temperatures approaching 2500°C, are not suitable at temperatures approaching 4000°C.

Metallic thermocouples, even though they exhibit desirable characteristics of size and stability, cannot withstand temperatures in excess of 2000°C and perform satisfactorily.

Radiation Pyrometers

Radiation pyrometers are temperature sensing devices which employ emitted radiation from the body whose temperature is being metered. There are four general classifications of radiation pyrometers, namely, optical pyrometers, total radiation pyrometers, photoelectric pyrometers and radiometers. (10) (14) (36)

A - Optical Pyrometers

Optical pyrometers are pyrometers which employ monochromatic spectral emission from the body in question. Most optical pyrometers operate at a

wave length of about 0.65 microns. This is due to the fact that the normal human eye is most sensitive to this wave length.

The "apparent" temperature of a body is determined by viewing the body through the lens arrangement of the pyrometer, and adjusting the current flowing through a filament, coincidental with the object, until the brightness of the filament and the brightness of the object are the same.

In determining the temperature of bodies emitting thermal radiation, an optical pyrometer will indicate an "apparent" temperature, which deviates from the true temperature. The deviation of the apparent temperature from the true temperature, is a factor of the emissivity of the surface being observed.

Since an energy viewed as coming from a body under study at the wave length of the pyrometer will cause the body to appear brighter, care must be taken to assure that only emitted radiation will be observed by the pyrometer. In working with blackbodies, the problem of reflected energy does not exist due to the fact that there is no reflected energy from a blackbody, however, gray bodies reflect a portion of the energy striking their surfaces. Metzger⁽²⁷⁾ utilized a mechanical discriminator to eliminate errors in temperature measurement due to reflectant energy.

There are two basic means by which the true temperature of a body may be determined with an optical pyrometer. First,⁽²⁷⁾ (10) the apparent temperature of the surface can be determined with an optical pyrometer, then using Wein's Law, and known data at $\lambda = 0.65\mu$, the true temperature

may be calculated. Secondly,⁽¹⁰⁾ some small specks of blackbody material may be imbedded in the surface of the body under observation, then using an auxiliary variable intensity light source, the true temperature of the object can be determined by changing the intensity of the light until the blackbody specks disappear when observed with the optical pyrometer.

Optical pyrometers are very flexible, and they can offer temperature measurements in excess of 5500°C (10,000°F).⁽¹⁰⁾ Further, the optical pyrometer is recognized as the standard temperature indicating instrument temperatures in excess of the gold point.⁽¹⁰⁾

B - Total Radiation Pyrometers

Total radiation pyrometers are temperature measuring devices which are intended to receive the entire amount of radiation from a given relative area on the surface of the object, whose temperature is to be determined. The radiant energy is used to activate a thermopile or vacuum thermocouple⁽³⁶⁾ to give an indication of the temperature of the surface. If, however, the emissivity of the surface is not unity, the temperature indicated by a total radiation pyrometer will be an "apparent temperature" which will be less than the true temperature of the surface under observation.

When a total radiation pyrometer is employed to determine the temperature of a surface, it is necessary that the pyrometer view only the surface under observation, due to the inherent characteristic that the pyrometer will indicate an average temperature over its field of view. The distance from the target to the receiver, as stated by Eckman⁽¹⁴⁾,

should not be greater than 10 to 20 times the maximum useful diameter of the target.

Additional characteristics associated with the total radiation pyrometer and its application are: although the entire radiant energy is ideally collected from the relative target area, most practical total radiation pyrometers utilize only the radiation between 0.1μ and 8.0μ ; absorbing or radiating media between the target and the receiver introduce errors in observed temperatures; further, in order to keep cold-junction compensation from necessary consideration, the receiver temperature should not be above 150°F .⁽³¹⁾

According to Hoge⁽²¹⁾ the total radiation pyrometer is most satisfactorily applied to the determination of temperatures in excess of 600°F (316°C). Hoge further states that there is no practical upper limit to the temperatures which can be measured. Another very desirable characteristic of the total radiation pyrometer is the instrument's speed of response.

Total radiation pyrometers are generally calibrated against a standard optical pyrometer.⁽¹⁰⁾

C - Photoelectric Pyrometers

A photoelectric pyrometer utilizes either a photoemissive tube or a photovoltaic cell to convert the radiant heat energy from a surface being viewed into electrical energy.

The photovoltaic cell produces directly an e.m.f. proportional to the amount of radiation received whereas the photoemissive tube produces an electron current proportional to the radiation received.⁽¹⁴⁾

Photoelectric pyrometers can be used satisfactorily in the range from 1500°F to 3000°F. At temperatures below 2000°F the use of an amplifier may be required due to the fact that the output of the photo-cell or phototube is too low to directly operate a potentiometer. (14)

Photoelectric pyrometer utilize radiation in the infa-red span of wave lengths, therefore, it is necessary to keep the instrument cool because the photo devices utilized do not have a stable response when the temperature of the cell or tube is in excess of 120°F.

The photoelectric pyrometer can be applied to many tasks due to its rapid response, simple and rugged construction, and need for no reference-junction and compensation. However, whatever the application may be, the instrument must be calibrated frequently. The calibration is usually performed in reference to a calibrated optical pyrometer.

A photoelectric pyrometer is subject to influency by the absorption of intermediate media as is the total radiation pyrometer. Also, the photoelectric pyrometer must view only the target in question. Corrections for transmission and emissivity cannot be readily calculated and therefore must be determined for each type of photoelectric instrument. This is due to the fact that neither monochromatic nor total radiation is utilized in the production of the e.m.f. and electron current.

D - Radiometers

Radiometers are very similar to total radiation pyrometers in that ideally they utilize the total radiation from a sample to give some type indication of the temperature of the sample, they differ in that no optical system is utilized. Several types of radiometers have been previously

described.

A miniature radiometer, as shown in Fig. 15, has recently been produced for application in the determination of temperatures in imaging furnaces whether they be solar furnaces or arc-image furnaces.

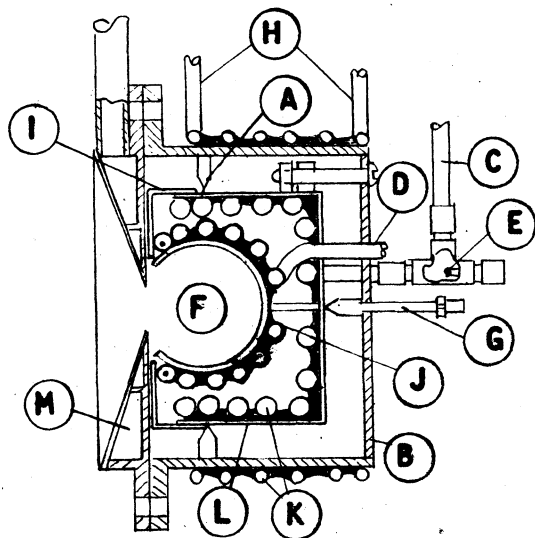
The unit is water-cooled and can therefore be utilized in reference to the continuous determination of temperatures developed by the highest radiation that can currently be produced. Further, the size of the instrument permits determination of flux distributions over regions of very steep gradient. (38)

"The instrument basically consists of a constantan foil fastened to an annular water-cooled copper heat sink. At the center of the circular foil diaphragm is fastened a copper wire. The resultant copper-constantan-copper-thermocouple provides an output proportional to temperature difference across radii of the foil. This e.m.f. has proved to be linear relative to thermal radiation rate". (38)

Calorimeters

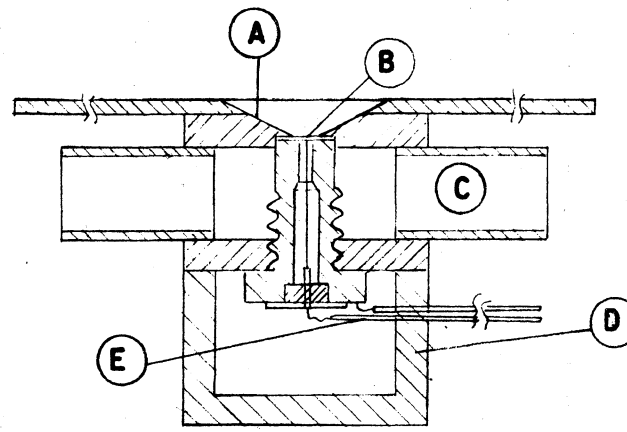
P. E. Glaser has recently developed a high radiation-flux, absolute, water-flow calorimeter, as shown in Fig. 16, for use in imaging furnaces. "This instrument can withstand flux-densities corresponding to blackbody temperatures up to 4000°C. It is an absolute, measuring calorimeter designed to reduce errors due to heat losses". (20)

"This instrument, based on the designs of calorimeters developed by Willoughby and Farber, provides a convenient means of measuring radiation flux. The calorimeter consists of a blackbody receiver provided with a conical aperture and contained in a cylindrical housing.



- | | |
|---------------------|------------------------------|
| (A) SPACER | (H) WATER CONNECTIONS |
| (B) OUTER CASE | (I) CYLINDER CLOSING CAP |
| (C) WATER INLET | (J) RECEIVER COOLING COIL |
| (D) WATER OUTLET | (K) CASE COOLING COIL |
| (E) THERMOPILE | (L) SHIELD |
| (F) RECEIVER | (M) APERTURE COOLING PASSAGE |
| (G) ADJUSTING SCREW | |

Figure 16. SECTION THROUGH ABSOLUTE CALORIMETER



- | |
|-------------------------------|
| (A) HIGHLY REFLECTIVE SURFACE |
| (B) FOIL DIAPHRAGM |
| (C) COOLING WATER PASSAGE |
| (D) THERMOCOUPLE LEADS |
| (E) OUTER CASING |

Figure 15. SECTION THROUGH MINITURE RADIOMETER

"Cooling water, which absorbs the heat flux entering the aperture and filling the inside of the blackbody receiver, first flows through coils around an inner cylinder acting as a radiation shield and then around the spherical receiver. Thermopiles consisting of two thermocouples each are installed in the water inlet and outlet for the measurement of required temperatures. Cooling water also circulates through the aperture shield, and over the cylindrical housing to reduce radiation heat transfer between the measuring section of the calorimeter and the ambient."(20)

"The blackbody receiver is a copper sphere; the inside of which has been blackened with Ebonol C, an oxidizing agent in an alkaline medium. The receiver is fitted inside a copper cylinder, centered by three glass beads and held in position by a zirconia rod. Thin-wall copper tubing is soft soldered to the inside cylinder and receiver. The inside cylinder is radially located by three pointed stainless steel spacers and held to the outer casing by two screws. A screw-in pointed spacer permits lateral adjustment. This arrangement minimizes heat losses by conduction or radiation to the outside casing.

"The aperture assembly is held to the outer casing by two flanges. The front of the aperture is conical, forming an angle of 140° so that the 120° (general) cone of radiation can enter the receiver.

"Cooling water is made to circulate through the aperture so that the edges nearest the focal zone will not melt. The cap closing the inner cylinder is plated with chromium and separated from the rear surface of the aperture. Thus, heat transfer by radiation from the aperture is reduced."(20)

"The probable error for this instrument is an estimated $\pm 5\%$. This error can be reduced by a more accurate means of measuring the water-flow rate and by a more sensitive temperature-measuring installation." (20)

III. THE INVESTIGATION

Object

The object of the investigation was to initiate research utilizing an arc-image furnace by developing an absolute calorimeter suitable for the determination of high intensity radiation flux over a relatively small surface area.

Design of Calorimeter

The calorimeter developed and utilized in this thesis consisted of four major components: (1) reflector, (2) receiver, (3) cooling coil, and (4) insulation. A description of each of these components follows.

Reflector

The reflector for the absolute, water-flow calorimeter was produced by machining a piece of cast brass to the dimensions indicated in Fig. 17.

An aperture of approximately $3/8$ inch was chosen because of three major considerations. First, since the arc mechanism required 16 mm anodes, an aperture significantly larger than $3/8$ inch would not have been completely filled by the image of the carbon arc. This would have given results not indicative of the flux being produced by the arc. Secondly, an aperture considerably smaller than $3/8$ inch would have introduced complications in the determination of the low amount of heat transferred. Therefore having only a small total heat transfer, any small errors in measurement would cause considerably more inaccuracy in radiation flux than the same measurement error with a large heat transfer. The final

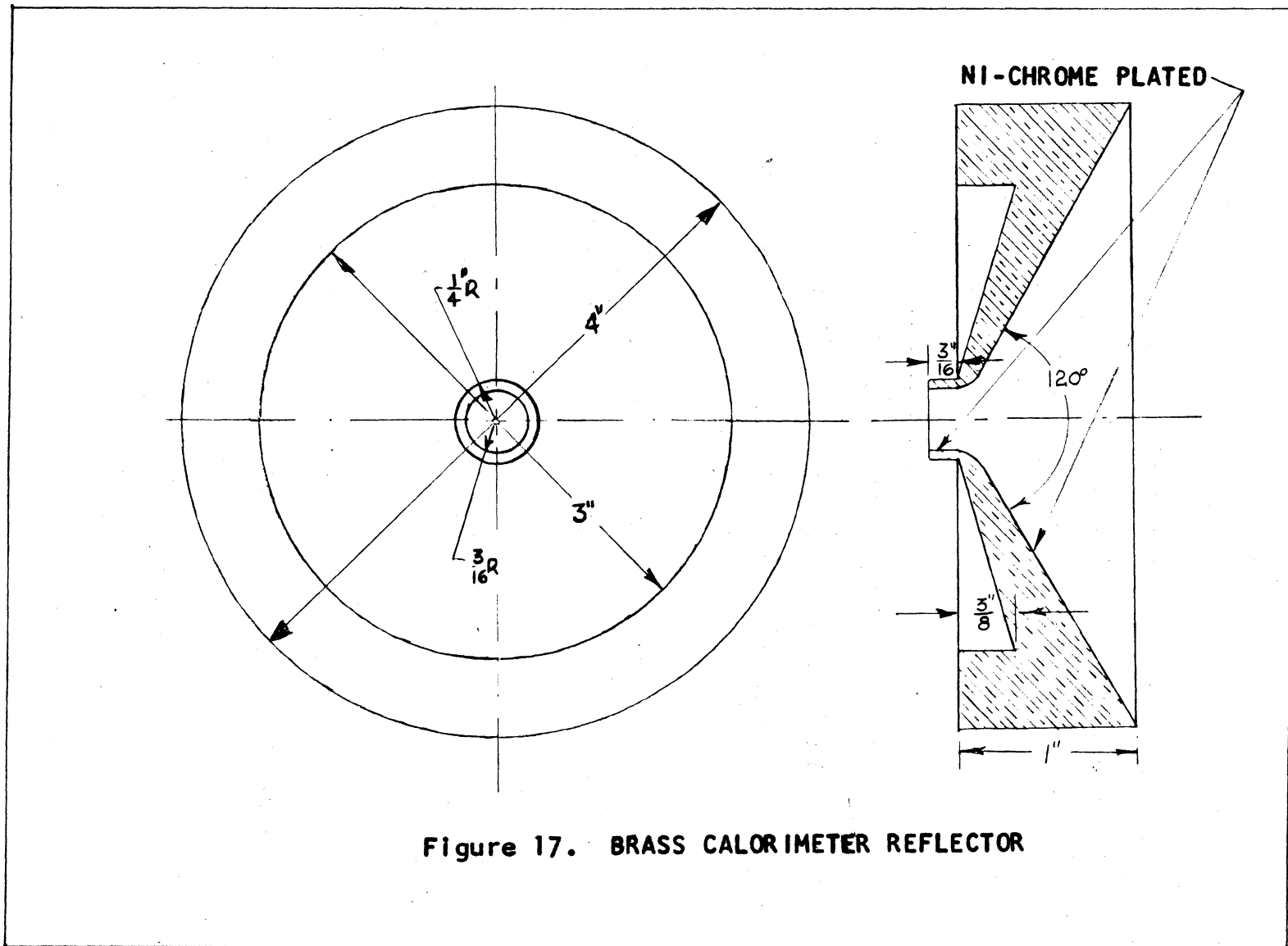




Fig. 17a. Brass Calorimeter Reflector

factor in the selection of the aperture diameter was the success which had been attained with a similar calorimeter using an aperture of 3/8 inch diameter by P. E. Glaser.⁽²⁰⁾

The conical recess in the reflector was chosen to have a solid angle of 120° . The reason for the selection of a 120° solid angle was that the radiation from the receiving reflector of the furnace converges toward the focal plane in a solid angle of 120° .

Brass, although it does not possess the high thermal conductivity of copper, was chosen for the reflector material because of its ease of machining.

Since it was known that a portion of the radiation would strike the cylindrical portion of the reflector aperture, the back of the reflector was recessed so that water could be passed through the reflector preventing damage to the reflector from the intense radiation during operation. In order that the reflector exhibit a minimum absorptivity, it was decided to first plate the reflector with 0.001 inch of nickel and then add 0.0001 inch of chromium plate. It was felt that the Ni-chrome plating would best withstand the high intensity radiation while exhibiting very high reflectivity.

Since the calorimeter was to be employed in conjunction with a miniature radiometer similar to the one previously described on page 60 having an overall diameter of four inches, the overall diameter of the reflector was chosen to be four inches so that the same supports could be used.

After the reflector had been constructed and plated, the aperture

was measured and found to have a diameter of 0.379 inch.

The reflector is pictured in Fig. 17a.

Receiver

It was desired that the receiver employed in the calorimeter have an optimum absorptivity. To this end, a graphical analysis was employed to evaluate the configurations of the receivers. The graphical analyses were based upon the convergence of 120° solid angle radiation produced by a point source of energy. An example of this analysis is shown in Fig. 18 for incident radiation rays at half-angles of 30° and 60° .

It is an accepted fact that a hollow sphere, having a radial entrance of small area relative to the total surface area, has an absorptivity most nearly approaching unity. The fabrication of a receiver having a spherical configuration and the connection of a cooling coil to the sphere presented problems which were too great to be undertaken in this investigation.

Preliminary analysis indicated that the simplest configuration, for ease of receiver fabrication, that most nearly approached blackbody cavity conditions, was a cylindrical receiver having a radial entrance, with a length to diameter ratio of approximately 1.5:1 or larger. This configuration, as illustrated in Fig. 19, was chosen to be used in the fabrication of receiver number one.

The procedure employed to evolve configuration number one, as previously mentioned, was graphical and based upon a point source of energy. In the actual application, the calorimeter will absorb energy produced by an arc having a finite area. Therefore, the radiation will not converge

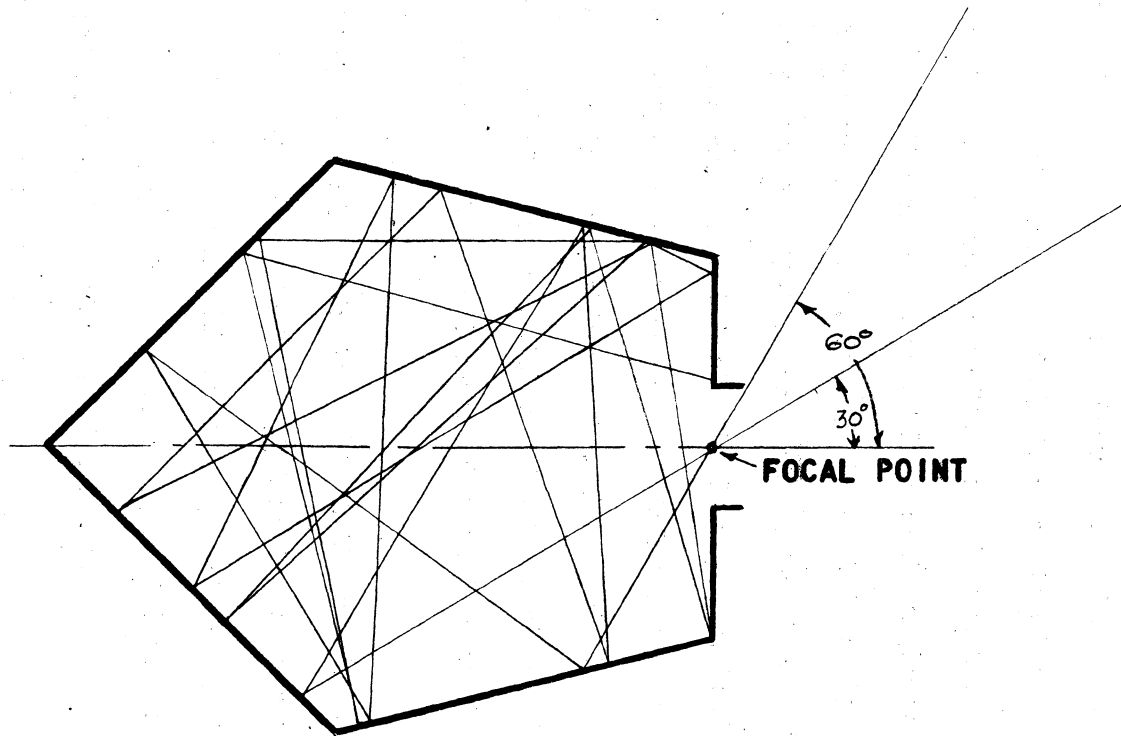
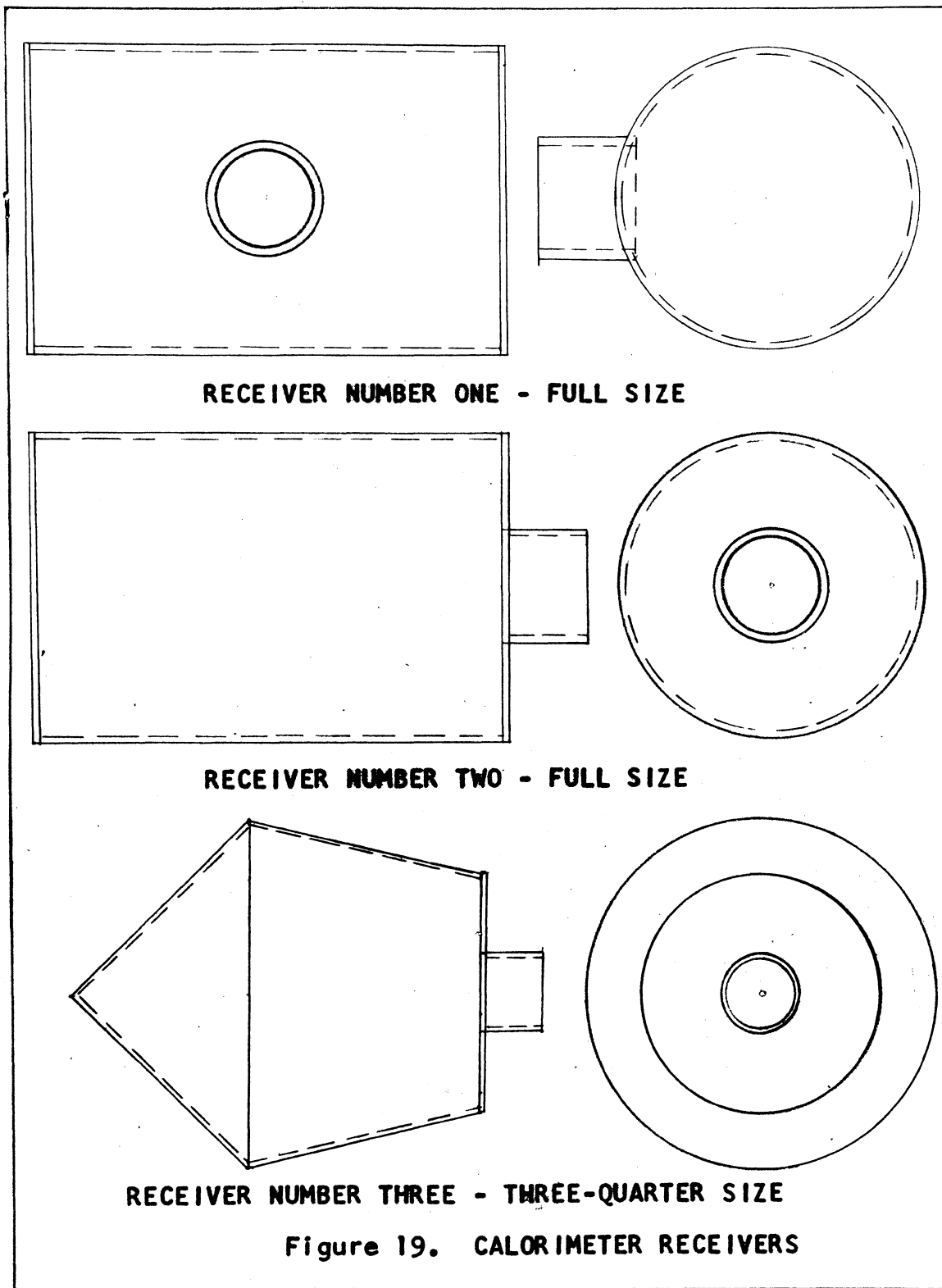


Figure 18. PARTIAL GRAPHICAL ANALYSIS
OF RECEIVER CONFIGURATION
AT 30° AND 60° INCIDENT RAYS



upon a point but, will form an image of the arc. Since the radiation does not converge upon a point, the actual angles of the incident rays will not be equal to the angles used in the graphical analysis. Some energy may be lost because of the reflection of radiation rays back through the entrance of the receiver.

It was decided to employ a cylindrical receiver, with the same dimensions as receiver number one, having an axial entrance as receiver number two, see Fig. 19. Graphical evaluation of the configuration of receiver number two indicated an absorptivity lower than the absorptivity of receiver number one because of the lesser number of reflections imposed upon incident radiation rays. Since, however, an arc of finite area was to be used as the energy source, it was felt that under actual operating conditions, the graphical evaluation might not be representative, and that receiver number two might perform more satisfactorily than receiver number one.

The configuration for receiver number three, as shown in Fig. 19, resulted from an investigation of modified mendenhall wedges. The analysis of trial and error configurations produced the basic configuration of receiver number three. Graphical analysis indicated that, with a point source of energy, the configuration amply approached blackbody conditions in that most radiation entering the receiver would be reflected a minimum of ten times. The internal surface area was made approximately equal to the internal surface area of receivers one and two so that errors would not result from size differential.

Since it was desirable for the receiver material to possess a high thermal conductivity, copper was chosen.

Since the overall diameter of the reflector was to be four inches, it was felt that the insulated receiver should not exceed four inches. It was determined that approximately 1/2 inch width would be needed for the cooling coil and insulation. Therefore, the maximum length of the copper pipe constituting the foundation for receiver number one was limited to three inches. Using a length to diameter ratio of 1.5:1, the diameter of the receiver was determined to be two inches. This also determined the dimensions of receiver number two because it was desired to compare the effect of radial and axial entrances to the same basic receiving chamber.

In order that the connected parts of each receiver remain fixed during the process of attaching the cooling coil to the receiver with lead solder, silver solder was used to fabricate the three receivers.

It was desired, that the calorimeter have a very high absorptivity, and it was also desired that the material used to cover the inner surface of the receivers be very easy to apply. To achieve both results, flat black paint having a recognized absorptivity in the range of 0.96 to 0.98 was used.

In order that a minimum amount of the radiation passing through the aperture of the reflector be lost, each receiver was fitted with a neck-piece 1/2 inch long and 5/8 inch in diameter. The desired effect of the neck-piece was the absorption of a portion of the radiation and the reflection of the radiation not absorbed directly into receiving chamber. The choice of dimensions for the neck-piece allowed for an air gap to exist between the receiver and the reflector in addition to allowing room for adequate insulation of the receiver.

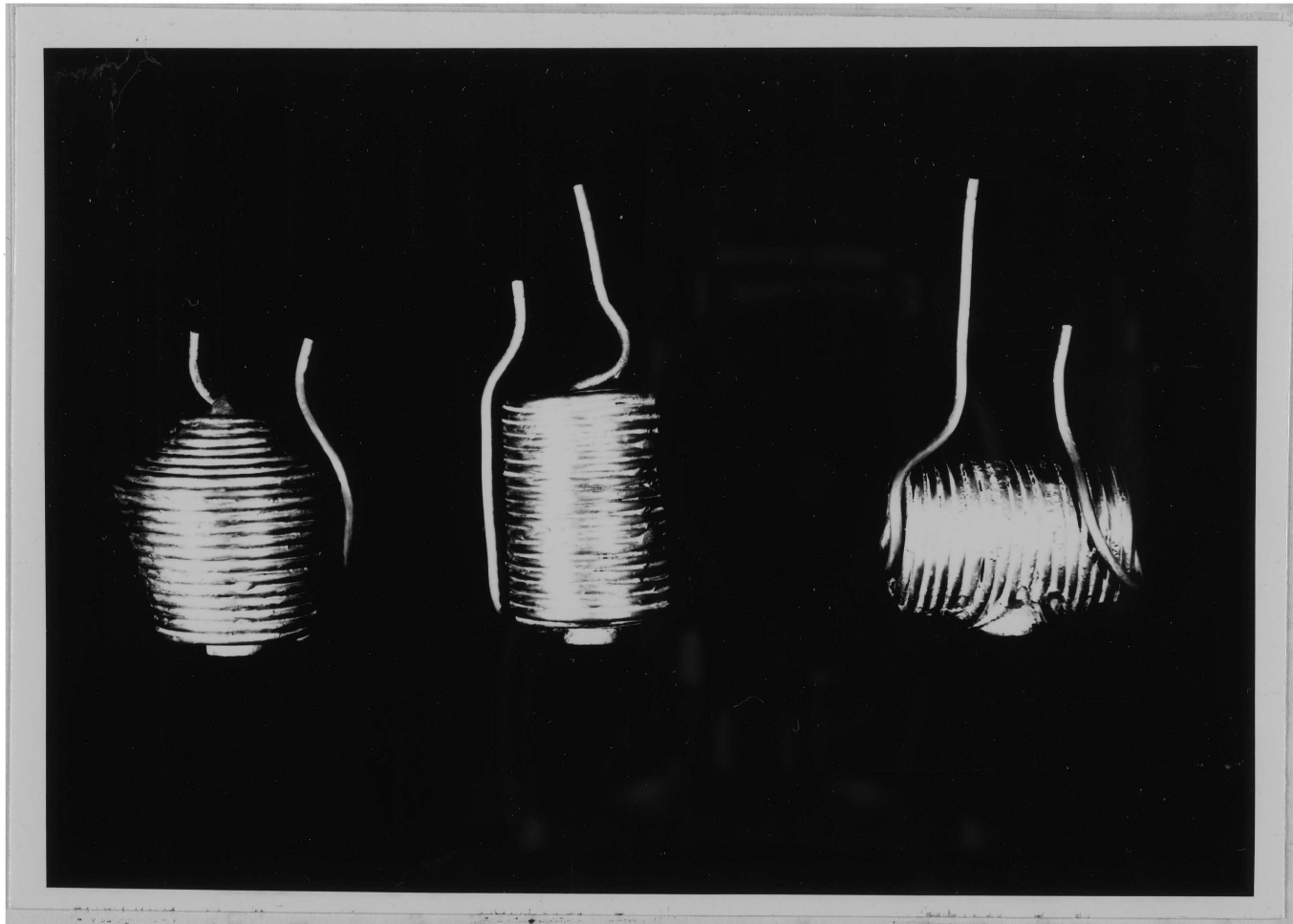
The three receivers tested in this investigation are pictured in Fig. 19a.

Cooling Coil

Initial analysis of the cooling of the receiver indicated that an annular arrangement of two walls for the passage of cooling water might be better than a helically wound copper cooling coil. This was due primarily to the anticipated problems of attaching the coil securely to all points on the receiver.

Further investigation revealed that for the maximum amount of heat to be transferred by the calorimeter to the cooling water, at the desired cooling water velocity and change in cooling water temperature, the mass flow of water would be so small that the width of the annulus would be approximately 0.0015 inch. At conditions of average radiation flux with the desired temperature rise in the cooling water, the velocity of the water would be too low for good heat transfer. Because of these considerations the application of an annular cooling water passage was considered impracticable.

Consequent analysis indicated that copper tubing in sizes from 1/8 inch to 1/4 inch would provide quite acceptable velocities at all anticipated amounts of radiation flux with the desired increase in cooling water temperature. It was determined that the pressure drop which would occur while using a 1/8 inch diameter coil would be too excessive, while the problem of attaching a coil having a 1/4 inch diameter would be too difficult. A coil having a diameter of 3/16 inch, however, was determined to have a reasonable pressure drop while not having significant



Receiver No. 3

Receiver No. 2

Receiver No. 1

Fig. 19a. Calorimeter Receiver with Cooling Coil

attachment problems.

It was decided that the cooling coil would be attached to the receiver by first coating the entire surface with solder, and then soldering the coil to the receiver as the coil was put into place. It was felt that this method would insure a positive contact between the cooling coil and the receiver.

It was anticipated that no temperature in excess of the melting point of lead would exist at any point in the receiver at any time. Therefore, due to its ease in application, lead solder was chosen to be used to make the connection between the cooling coil and the receiver.

In order to clarify the relative positions of the reflector, receiver, and cooling coil, a partial assembly of the calorimeter is shown in Fig. 20.

Insulation

Each of the three receivers was insulated by first covering all exterior surfaces with approximately 1/8 inch of 85% magnesia insulation. Finally, each receiver was enclosed in a galvanized sheetmetal container which was packed with fiber glass.

The combination of both magnesia and fiber glass was felt to be sufficient to reduce any heat exchanges with the surroundings to insignificant quantities.

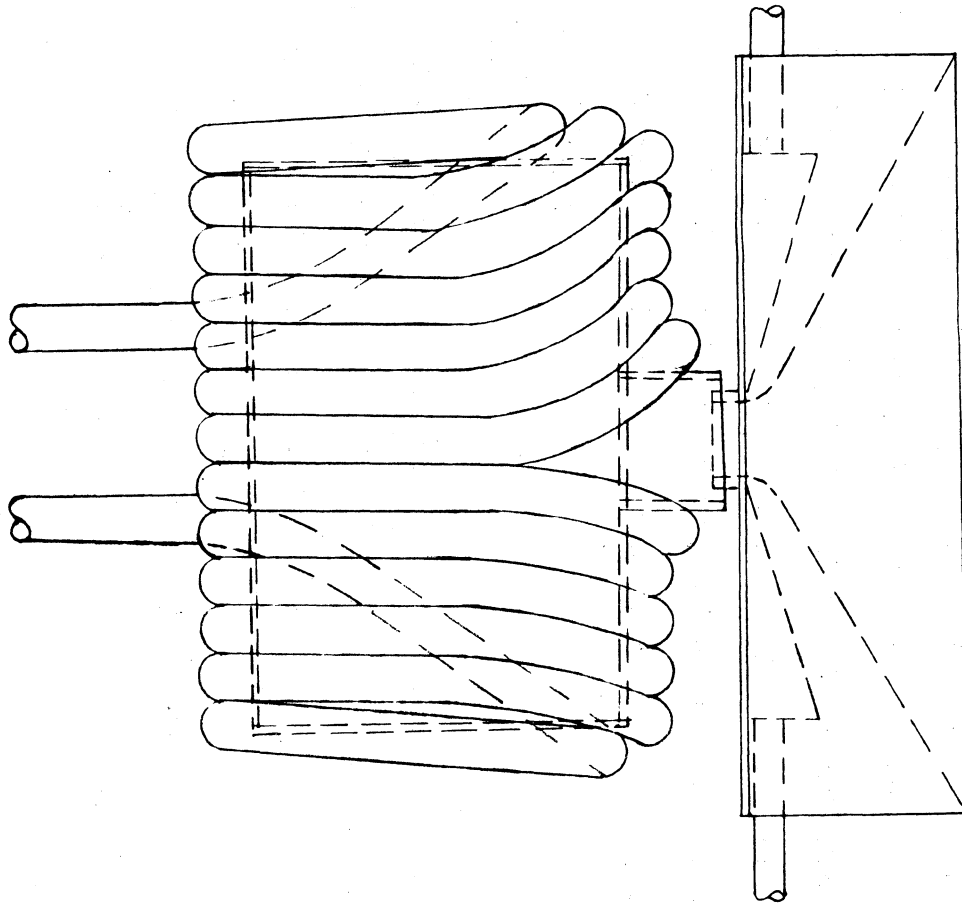


**Figure 2o. PARTIAL ASSEMBLY OF CALORIMETER
(INSULATION NOT SHOWN)**

List of Apparatus

To facilitate association of the items utilized in this investigation, three classifications of apparatus will be used. They are as follows:

- (1) Operating Apparatus
- (2) Testing Apparatus
- (3) Tested Apparatus

OPERATING APPARATUS

Arc-Image Furnace: An arc-image furnace consisting of two 60" General Electric Search Lights, Model No. 1942, Serial Nos. 60541 and 59244. Used to supply high intensity radiation flux.

Carbon Electrodes: Surplus government 16 mm carbon anodes and 11 mm carbon cathodes obtained from Publicity Searchlight Company, New York, New York. Used as electrodes for the aforementioned furnace.

Motor Generator Unit: General Electric Motor-Generator Unit, Model No. 35G554, Serial No. 7112524 rated at 250 hp at 125 volts D.C. and 600 amps. Shunt wound. Used to supply electrical power to arc-image furnace.

TESTING APPARATUS

Potentiometer: Portable semi-precision Leeds and Northrup potentiometer Serial No. 1134182, range 0 - 16 mv and 0 - 80 mv used to determine the electromotive force produced by thermocouples at various positions within the calorimeter and reflector cooling water connections and to calibrate the thermocouple wire.

Thermocouples: Minneapolis-Honeywell No. 9B1C4 matched copper constantan thermocouple wire No. 24 gauge. Thermal junctions produced in the mechanical engineering instrumentation laboratory by oil-cooled arc fusion process.

Used to determine cooling water temperatures at various positions.

Platform Scales: Fairbanks platform scales No. 39, range 0 to 20 pounds with one ounce divisions, 0 to 100 pounds. Used to determine the mass flow of receiver cooling water.

Platform Scales: Montgomery-Ward and Company platform scales No. 2 range 0 to 50 pounds in quarter pound divisions. Used to determine the approximate mass flow of reflector cooling water.

Stopwatch: Meylan stopwatch, Serial No. 307390, range 0 to 15 minutes in 0.1 second divisions. Used to determine the flow rates of cooling water.

Micrometer: Starrett micrometer Model No. 203, range 0 to 1 inch in 0.001 inch divisions. Used to determine the diameter of the reflector aperture.

Thermometer: Fisher No. 11 nitrogen filled thermometer Bureau of Standards No. 49105, range 17.8 to 30.2°C in 0.02°C divisions. Used to calibrate thermocouple wire.

Thermometer: Fisher thermometer range 0 to 230°F in 2°F divisions. Used to obtain room temperature.

Thermosbottle: Good quality vacuum thermosbottle with cork plug. Used to hold ice bath.

Ice Bath: Ice and water contained in the aforementioned thermosbottle. Used to obtain 32° reference junction temperature.

TESTED APPARATUS

Calorimeter Receivers: Three in number, copper construction. Built in the mechanical engineering shop. Used to determine the radiation flux passing through the reflector aperture.

Reflector: Brass material, four inch overall diameter, 0.379 inch aperture diameter built by Mechanical Development Company, Salem, Virginia. Plated by Norfolk and Western Railway Company, Roanoke, Virginia. Used to shield receiver from undesirable radiation.

Reflector Holder: Steel construction, built by the mechanical engineering shop. Used to hold the reflector at the proper position with respect to the receiving furnace reflector.

Operational Procedure

In order to serve as a guide for other investigators, the apparatus used in the investigation is shown schematically in Fig. 21 and the procedure for the use of the calorimeter in determining radiation flux will be broken into steps, which are as follows:

1. Open valve, K, on 3/4" main water line to flush stagnant water from line. Allow to run so that equilibrium of line water temperature can be quickly obtained.
2. While flushing water line, check the arc-image furnace to insure that both furnace reflectors A and P are at the following positions:
Sender, A: Azimuth: 0° Elevation: -15 mills
Receiver, P: Azimuth: -0.5° Elevation: +35 mills
3. Check control rods, B, from arc control box, D, to insure freedom of movement, then install electrodes, C, so that the anode protrudes 11/16" from the nose cap. The position of the cathode is not of primary concern because it will be advanced by the automatic arc-strike controls until the arc is struck.
4. Install the calorimeter reflector, O, and holder such that the center of the aperture is 6.0" above the top of the calorimeter support. This mounting can easily be checked later.
5. Shut off valve K, and connect the 1" main cooling water hose to the valve K; connect the small plastic hose to the copper tubing on reflector, O; then, open petcock, L.
6. Check to insure that the receiver cooling water petcock, M, is closed, then open valve, K, on the main water line. Allow to run.

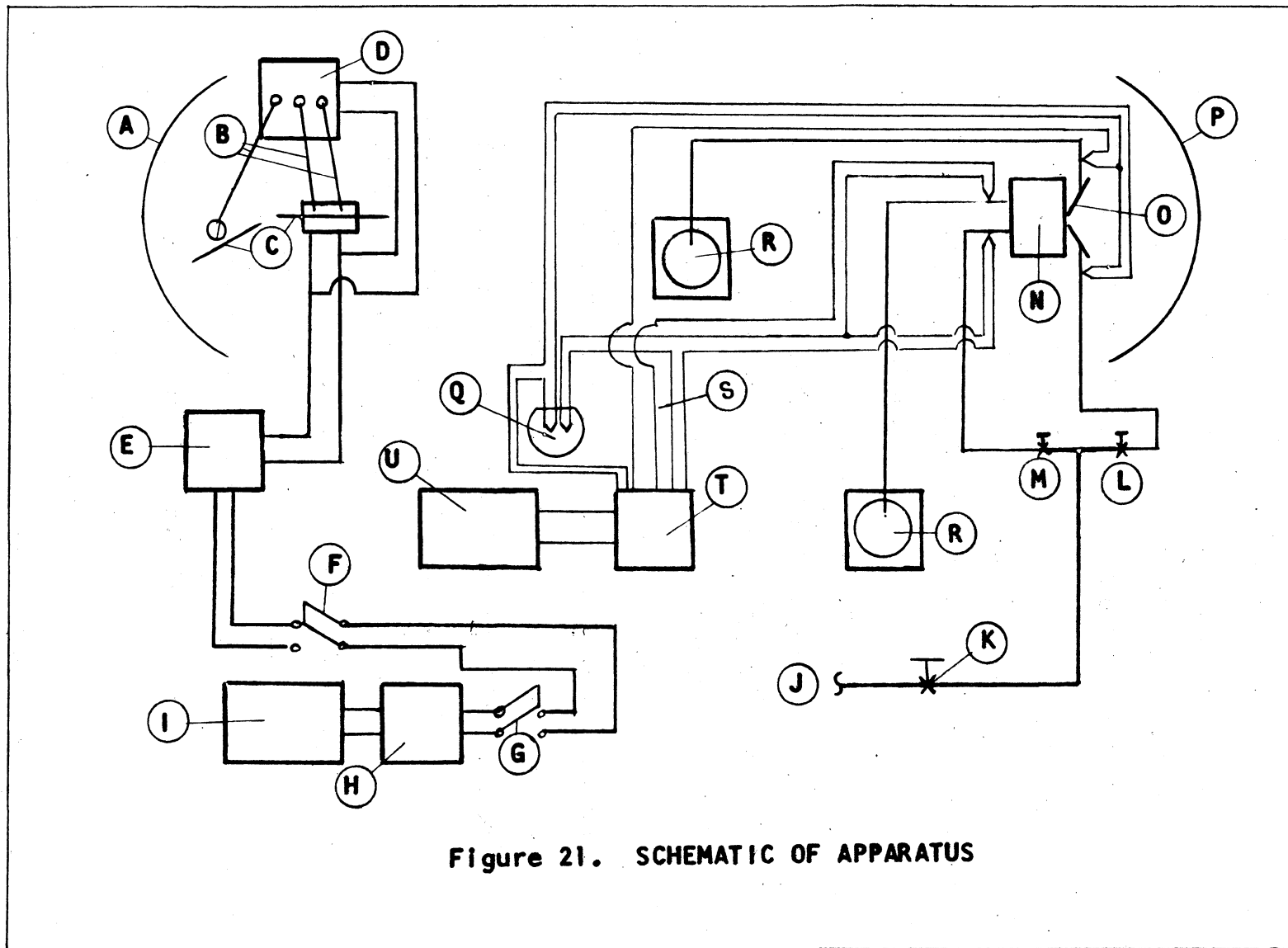


Figure 21. SCHEMATIC OF APPARATUS

LEGEND FOR Figure 21

- | | |
|----------------------------|-----------------------------|
| (A) SENDING REFLECTOR | (L) REFLECTOR PETCOCK |
| (B) ARC CONTROL RODS | (M) RECEIVER PETCOCK |
| (C) CARBON ELECTRODES | (N) RECEIVER |
| (D) ARC CONTROL BOX | (N) REFLECTOR |
| (E) CONTROL SWITCH BOX | (P) RECEIVING REFLECTOR |
| (F) SEARCHLIGHT SWITCH | (Q) ICE BATH |
| (G) MOTOR-GENERATOR SWITCH | (R) SCALES AND WEIGH TANK |
| (H) EXCITER | (S) THERMOCOUPLE LEADS |
| (I) MOTOR-GENERATOR SET | (T) THERMOCOUPLE SWITCH BOX |
| (J) MAIN WATER LINE | (U) POTENTIOMETER |
| (K) MAIN WATER VALVE | |

7. While flushing the cooling water line and the reflector, energize the 250 horsepower motor-generator, I, set in the Internal Combustion Laboratory and set the voltage at 84 volts by adjusting the rheostat on the exciter, H. Allow to run.
8. Throw switch, G, in the exciter cage to the 250 horsepower position. This routes the power generated to the searchlight switchbox. Then throw switch, F, to the searchlight position. This supplies power directly to the arc-image furnace.
9. Adjust the calorimeter support until the double-pointed indicator on the support is collinear with the line indicating the position of maximum flux.
10. Check to insure that cooling water is flowing through the reflector, then, throw the control switch, E, to the "on" position. This energizes the electrodes, C, and arc control box, D, and an arc will automatically strike.
11. Adjust the position of the arc by movement of the handwheel on reflector, A, until the tip of the anode is collinear with the black line on the ground glass viewer on reflector, A. When the tip of the anode is on the black line, the arc is being formed at the focal plane of the sending parabolic reflector, A. Check anode feed rate, and adjust the anode feed rate control on the arc control box, D, if necessary to maintain the proper anode position.
12. Put on a welders helmet then switch off the arc-image furnace and immediately look into the aperture of the reflector, O. An image of the anode should appear through the aperture of the reflector. If an image does not appear properly, check the initial settings and make

the necessary corrections.

13. Hook up the leads from the thermocouple switchbox, T, to the potentiometer, U; place cold junctions in the ice bath, Q; then check the thermocouples to insure that all junctions are still intact.
14. Connect the plastic cooling water lines to the cooling coil on the receiver, N; then open petcock, M. Stop all leaks in exit line connections and minimize all leaks in inlet water connections. Install radiation shields around cooling water connections.
15. Set the receiver, N, in a position such that the entrance is concentric with the aperture protuberance of the reflector, O. There should be approximately 1/16" between the copper plate on the after portion of the reflector and the receiver sheet metal container. It has been found that the position of the receiver relative to the reflector is not altered during calorimeter movement. However, if desired, the receiver can be mounted semi-permanently into its position relative to the reflector.
16. Check scales, R, to determine if they are functioning properly, then direct cooling water flows into the weigh tanks.
17. When the cooling water temperature becomes constant, the arc-image furnace can be energized by throwing the control switch to the "on" position.
18. With the furnace in operation, frequently check the differential EMF of the receiver thermocouples until the value becomes constant. When the differential EMF becomes constant, a test run can be made.
19. Set a weight on the receiver cooling water scales and when balance

- occurs, start the stopwatch.
20. Set a new larger weight on the scales and wait for balance to occur. While waiting for balance, frequently check differential EMF for the receiver and reflector, incoming water thermocouple EMF, arc position and make an approximate determination of the cooling water flow rate. Then read and record room temperature. When using a total flow of 10 pounds of receiver cooling water, sufficient time exists for all items indicated above.
 21. When balance occurs, stop the watch and record receiver differential EMF, inlet water EMF, total receiver cooling water flow, time required, reflector differential EMF and approximate reflector cooling water flow rate.
 22. The calorimeter can now be moved to any new position desired. If a run is desired at one of the positions used in the flux distribution test, that position can be correctly set by rotating the handwheel on furnace reflector, P, until when looking through the access opening below the handwheel the double-pointed indicator is aligned with the position mark desired. The use of a double point on the indicator avoids parallax.
 23. Upon completion of the desired testing, de-energize the furnace by returning the arc-control switch, E, to the "off" position. Turn off cooling water valve, K. If desired, disconnect cooling water lines and remove the calorimeter. Return searchlight switch, F, to the neutral position. Return motor-generator switch, G, to the neutral position. De-energize the motor-generator set and exciter.

24. Sufficient time should have now elapsed for the replacement of the carbon electrodes if necessary. If the furnace has been in operation for two hours, continuous or intermittent, a small amount of 30 weight motor oil should be placed on bearings and gears for lubrication and cooling.

Data and Results

The experimental investigation was conducted in three series, namely:

1. Receiver Test Series
2. Reflector Test Series
3. Flux Distribution Test Series

A discussion of each of these test series, the data obtained, and the results computed from the data follows.

Receiver Test Series

The primary object of this series of tests was to determine which of the three receivers had the maximum absorptivity of thermal radiation. The exact position of the calorimeter relative to the base position, or position of minimum radiation flux as indicated by the position marked "0" on the calorimeter support, was of no prime importance. Therefore, the four positions used in this series of tests were taken at random.

After the steps necessary to check the proper calorimeter alignment had been taken, the test was begun by positioning the calorimeter near the optimum point, or point of maximum radiation flux. With the calorimeter in this position, the radiation flux was measured with each of the three receivers in the calorimeter. Three similar sets of measurements were made at positions successively nearer the base position.

The data obtained from the receiver test series and the results of this data are presented in Table I.

Reflector Test Series

During preliminary operation and during the receiver test series, it was quite apparent, from the temperature rise of the cooling water,

DATA AND RESULTS

Positions*	Receiver Number	Water Flow (lbs)	Time (min-sec)	Receiver EMF		Receiver ΔEMF (mv)	Temperature Rise Through Radiation		% of Maximum
				In (mv)	(°F)		Receiver °F	Flux (Btu/hr-ft ²)	
A	1	10	7 - 54.9	0.893	(73.0)	0.278	12.3	1.19 x 10 ⁶	-
	2	10	6 - 40.9	0.897	(73.1)	0.225	9.8	1.13 x 10 ⁶	95
	3	10	7 - 54.6	0.895	(73.1)	0.270	12.0	1.17	98
B	1	10	5 - 55.2	0.882	(72.4)	0.203	8.9	1.15 x 10 ⁶	-
	2	10	5 - 58.3	0.885	(72.6)	0.195	8.5	1.09 x 10 ⁶	95
	3	10	7 - 16.4	0.887	(72.7)	0.234	10.7	1.13	98
C	1	10	5 - 46.6	0.920	(74.2)	0.175	7.4	9.86 x 10 ⁵	-
	2	10	7 - 42.4	0.921	(74.3)	0.216	9.4	9.36 x 10 ⁵	95
	3	10	7 - 53.2	0.922	(74.3)	0.200	8.6	9.66	85
D	1	10	8 - 54.6	0.895	(73.1)	0.217	8.4	7.25 x 10 ⁵	-
	2	10	10 - 13.7	0.904	(73.5)	0.212	9.2	6.88 x 10 ⁵	95
	3	10	10 - 07.7	0.903	(73.5)	0.215	9.3	7.10 x 10 ⁵	98

Room Temperature: 84°F Arc Voltage: 78 Volts D.C. Arc Current: 150 Amps

*Positions taken at random with respect to the base position of the calorimeter.

TABLE I. RECEIVER TEST SERIES

that the calorimeter reflector was absorbing a large amount of thermal radiation. Therefore, it was advisable to determine what approximate effect various reflector cooling water flow rates imposed upon the absorption of heat by the reflector. It was decided to run a series of tests with the calorimeter at one position, during which, the flow rate of reflector cooling water could be varied.

After checking the calorimeter, it was positioned near the optimum point. With the calorimeter in position, a set of measurement of the approximate flow rate of cooling water and the temperature rise of the cooling water as it passed through the reflector was made.

Three other similar sets of measurements were made at various flow rates which were regulated by manipulation of the valve on the main water line.

The data obtained from this series of tests and the results of this data are presented in Table II.

Flux Distribution Test Series

It was felt that some knowledge of the flux distribution of the arc-image furnace would be beneficial to future investigations. Therefore, it was decided to determine the radiation flux at 0.50 inch intervals from the base position until the optimum point had been passed.

After checking the alignment of the calorimeter, it was moved to the base position. A set of measurements necessary to determine the radiation flux at that point was taken. After securing the data, the calorimeter was successively moved to positions 1, 2, 3, and 4, where similar measurements were made. As the calorimeter was being moved from position

DATA AND RESULTS						
Run Number	Reflector Water Flow (lbs)	Time (min - sec)	Reflector EMF In (mv) (°F)	Reflector ΔEMF (mv)	Temperature Rise Through Reflector °F	Heat Absorbed Btu/min
1	5	0 - 38	0.955 (75.8)	0.078	3.4	27.0
2	5	0 - 52.7	0.945 (75.4)	0.109	4.7	27.3
3	5	0 - 32.9	0.905 (73.6)	0.065	3.0	27.2
4	5	0 - 42.1	0.882 (72.4)	0.082	3.8	27.2
Room Temperature: 85°F Arc Voltage: 78 Volts D.C. Arc Current: 150 Amps						

TABLE II. REFLECTOR TEST SERIES

4 toward position 5, the differential EMF of the receiver cooling water began to decrease, thereby indicating the optimum point had been passed. The point of maximum intensity was then located by very slowly moving the calorimeter until the receiver cooling water thermocouples were producing the maximum differential EMF. After locating the optimum point a set of measurements was taken to determine the radiation flux at that point. After the measurements were taken, the furnace was shut down, and the distance from the base position to the optimum point was determined to be 1.84 inches.

The furnace was allowed to cool for approximately one hour, then using a different pair of electrodes and a different flow rate of cooling water, a series of runs was made to determine if reproduction of results was possible.

The data obtained from this series of tests and the results from this data are presented in Table III.

In order to clarify the results as presented in Tables I, II, and III, a set of sample computations follows.

DATA AND RESULTS

Position	Water Flow (lbs)	Time (min - sec)	Receiver In (mv) (°F)	Receiver ΔEMF (mv)	Temperature Rise Through Receiver °F	Heat Absorbed Btu/min	Radiation Flux - Ave. Btu/hr-ft ²	Equivalent Blackbody Temperature °R
Base or 0	10	7 - 36.6	0.868 (71.7)	0.015	0.7	0.94	7.21 x 10 ⁴	2500
	10	5 - 44.4	0.855 (71.1)	0.011	0.5	0.94		
- 1 - 0.50" from 0	10	7 - 36.8	0.868 (71.7)	0.020	0.9	1.23	9.44 x 10 ⁴	2700
	10	5 - 44.8	0.855 (71.1)	0.014	0.7	1.23		
- 2 - 1.00" from 0	10	7 - 30.8	0.870 (71.7)	0.050	2.4	3.20	2.46 x 10 ⁵	3450
	10	5 - 43.3	0.855 (71.1)	0.038	1.9	3.22		
- 3 - 1.50" from 0	10	7 - 27.8	0.870 (71.8)	0.205	9.1	12.2	9.45 x 10 ⁵	4850
	10	5 - 42.0	0.855 (71.1)	0.150	7.0	12.2		
- 4 - 2.00" from 0	10	7 - 22.0	0.875 (72.1)	0.280	11.5	15.6	1.21 x 10 ⁶	5150
	10	5 - 45.6	0.855 (71.1)	0.201	9.0	15.6		
Optimum: 1.84" from 0	10	7 - 20.0	0.875 (72.1)	0.290	13.4	17.6	1.35 x 10 ⁶	5300
	10	5 - 41.0	0.855 (71.1)	0.226	10.0	17.6		
	10	7 - 25.2	0.872 (71.9)	0.292	13.0	17.6		

Room Temperature: 80°F Arc Voltage: 78 Volts D.C. Arc Current: 150 Amps

TABLE III. FLUX DISTRIBUTION TEST SERIES

IV. SAMPLE COMPUTATIONS

The following computations were based upon run number two for the determination of the radiation flux at the optimum point.

1. Cooling water flowrate: \dot{m}

$$\dot{m} = \frac{M}{T}$$

where: M = total flow of cooling
water, lbs.

T = total time for flow, min.

$$= \frac{(10 \text{ lbs.})}{5 \text{ min.} + (42.0 \text{ sec.}/60 \text{ sec./min.})}$$
$$= \frac{10 \text{ lbs.}}{5.68 \text{ min.}}$$

$$\dot{m} = 1.76 \text{ lbs/min}$$

2. $EMF(\text{receiver out}) = EMF(\text{receiver in}) + \Delta EMF(\text{receiver})$

where: $EMF(\text{receiver out})$ = electro-
motive force produced by
thermocouple in line at
cooling water exit.

$EMF(\text{receiver in})$ = electro-
motive force produced by
thermocouple in line at
cooling water entrance.

$\Delta EMF(\text{receiver})$ = differential
electromotive force produced
by differential thermocouple

in cooling water line.

$$= 0.855 \text{ mv} + 0.226 \text{ mv}$$

$$\text{EMF}(\text{receiver out}) = 1.081 \text{ mv}$$

3. Cooling water temperature rise, Δt

$$\Delta t = t_{\text{out}} - t_{\text{in}}$$

where: t_{out} is determined from thermo-couple calibration curve at

$$\text{EMF}(\text{receiver out}) = 1.081 \text{ mv.}$$

t_{in} is also determined from calibration curve at

$$\text{EMF}(\text{receiver in}) = 0.855$$

$$= 81.1^\circ\text{F} - 81.1^\circ\text{F}$$

$$\Delta t = 10.0^\circ\text{F}$$

4. Aperture area, A_a

$$A_a = \frac{\pi D^2}{4}$$

where: D = diameter of aperture

$$= \frac{\pi (0.379 \text{ in.})^2}{4 (12 \text{ in./ft.})}$$

$$A_a = 7.82 \times 10^{-4} \text{ ft.}^2$$

5. Heat transfer rate, q

$$q = \dot{m} C_p \Delta t$$

where: C_p = specific heat of water

$$= (1.76 \text{ lbs./min.}) \left(\frac{1 \text{ Btu}}{\text{lb.} \cdot ^\circ\text{F}} \right) (10.0^\circ\text{F})$$

$$q = 17.6 \text{ Btu/min.}$$

6. Radiation flux, Q

$$Q = 60 \frac{q}{A_a}$$
$$= \frac{(60 \text{ min./hr.}) (17.6 \text{ Btu/min.})}{7.82 \times 10^{-4} \text{ ft.}^2}$$
$$Q = 1.35 \times 10^6 \text{ Btu/ft.}^2 - \text{hr}$$

7. Equivalent blackbody temperature, T_b

$$T_b = \left(\frac{Q}{\sigma} \right)^{1/4}$$

where: σ = Stefan-Boltzmann constant

$$= \left(\frac{1.35 \times 10^6 \text{ Btu/hr.-ft.}^2}{0.1714 \times 10^{-8} \text{ Btu/hr.-ft.}^2\text{-}^\circ\text{R}^4} \right)^{1/4}$$

$$T_b = 5300^\circ\text{R}$$

8. Combined efficiency, ζ_c

$$\zeta_c = \frac{(q_T) (1000) (60)}{(V) (C) (3413)}$$

where: q_T = estimated total heat absorbed
by calorimeter.

V = arc voltage.

C = arc current

$$= \frac{(45 \text{ Btu/min.}) (1000 \text{ watt/KW}) (60 \text{ min./hr.})}{(78 \text{ volts}) (150 \text{ amps}) (3413 \text{ Btu/KW-hr.})}$$

$$\zeta_c = 0.068 \text{ or } 6.8\%$$

V. DISCUSSION

In order to formulate conclusions resulting from the data obtained in the three series of tests, the discussion of results will be presented in the following sections:

1. Receiver Test Series
2. Reflector Test Series
3. Flux Distribution Test Series
4. Other Pertinent Information from all Test Series

Receiver Test Series

The results of this test series as presented in Table I prove conclusively that receiver number one had the maximum absorption of thermal radiation. The absorptivity of receiver number two remained constant at 95% of the absorptivity of receiver number one, while receiver number three maintained an absorptivity essentially 98% of the absorptivity of receiver number one.

The graphical analysis of receiver two, as previously mentioned, indicated a lower absorptivity than that of receiver one, and as the results indicate, its absorptivity was actually 5% less than that of receiver number one. This, therefore, supports the use of the graphical analysis of receiver configurations to some extent. It must be noted, however, that the graphical analyses used were based on smooth interior surfaces. No determination of the condition of the interior surface could be made. However, it is postulated that the surfaces are fairly smooth and free of proturbations, large paint runs, etc. Therefore, it is concluded the configuration was the limiting factor upon the absorp-

tivity of the receiver.

Receiver number three exhibited an absorptivity less than anticipated (approximately 2% less than number 1.) Since it was designed on a modified wedge basis with a high number of reflections being imposed on incoming radiation waves, its absorptivity should have more closely approached that of receiver number one. There are two possible causes for the smaller absorptivity than anticipated. First, the construction of the receiver was such that the surface of each section was not as smooth as desirable. Secondly, during fabrication of receiver, it is quite possible that the angles between each section and its adjoining sections were slightly in error. It was hoped that the surface condition would increase the absorptivity of the receiver, however, it is possible that the absorptivity of the receiver was reduced by the reflection of radiation back out the receiver entrance because of either the surface condition or error in configuration angles.

It should be noted that the low absorptivity, 85%, of receiver number three in run number three was anticipated before sample computations were completed. It was discovered, immediately upon completion of the run, that the arc was not being formed at the focal point in the arc-image furnace. With the arc not being formed at the focal point of the arc-image furnace, a reduction in radiation flux going into the calorimeter resulted.

Since the materials used in the construction, cooling, insulating and surface coating of each of the three receivers were the same, the results from this test series are considered valid.

It was decided, therefore, to use receiver number one as the permanent calorimeter receiver because of its superior performance.

Reflector Test Series

As previously stated, this series of tests was directed at the determination of the varying effect of various reflector cooling water flow rates upon the performance of the calorimeter. The results as presented in Table II prove conclusively that the heat absorption of the reflector at any calorimeter position is constant within the accuracy of the instrumentation used.

At the position used for this test, the four test runs gave a range of reflector heat absorption of from 27.0 Btu/min to 27.2 Btu/min. The reflector cooling water flow rates were varied from approximately 5 lb/min to approximately 10 lb/min as it was anticipated that such a range of cooling water flow rates might be utilized during subsequent investigation.

It is felt that since the deviation of the maximum heat absorption from the minimum heat absorption is less than 1%, the results are valid.

It should be noted, however, that since the heat absorption of the reflector is approximately two times that of the receiver, further study of the reflector is warranted.

Flux Distribution Test Series

As presented in Table III, the results of this test series show that quantities of radiation flux of 7.21×10^4 Btu/hr-ft², 9.44×10^4 Btu/hr-ft², 2.46×10^5 Btu/hr-ft², 9.45×10^5 Btu/hr-ft², 1.21×10^6

Btu/hr-ft² and 1.35×10^6 Btu/hr-ft² were measured at positions 0, 1, 2, 3, 4, and optimum point respectively. The flux distribution of the furnace is also presented graphically in Fig. 22.

As previously stated, a second group of runs were made to determine if the results of the first group were reproducible. The results of the first group of tests as shown in Table III in the heat absorbed column were reproduced almost exactly in the second group of tests. At the base position, the second test showed a heat absorption of essentially 0.94 Btu/min. Compared with a value of 0.94 Btu/min from the first run, the comparison of first run results to second run results for positions 1, 2, 3, and 4 are 1.23 Btu/min to 1.23 Btu/min, 3.20 Btu/min to 3.22 Btu/min, 12.2 Btu/min to 12.2 Btu/min, and 15.6 Btu/min to 15.6 Btu/min respectively. In positions 1, 3, and 4, the reproduction was 100% while in position 2, the reproduction was 99.4% which is well within the limits of acceptable reproduction of results. At the optimum point, two sets of measurements were taken to compare with the first set. The results of runs two and three both show values for the heat absorbed of 17.6 Btu/min. In the first run, the heat absorbed was also 17.6 Btu/min, therefore, 100% reproduction of results was experienced at the optimum point.

It should be noted, however, that the accuracy of the thermocouples is limited to only $\pm 0.1^\circ\text{F}$ and that the potentiometer used in conjunction with the thermocouples is accurate to only ± 0.005 mv, which corresponds to 0.15°F . In view of these limitations upon temperature measurement, the results, as presented, are considered accurate to two or three

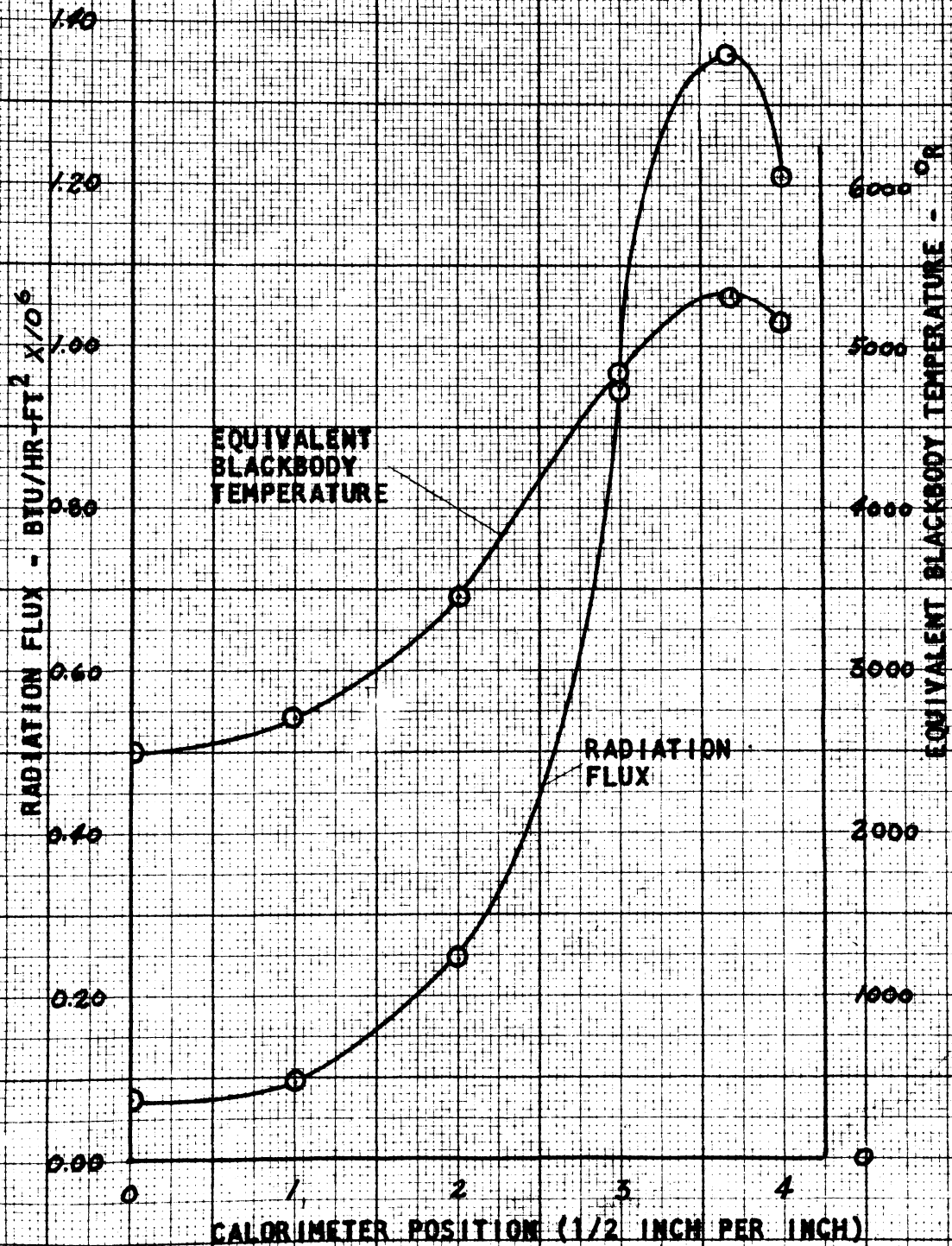


Figure 22. ARC-IMAGE FURNACE FLUX DISTRIBUTION AS MEASURED BY CALORIMETER

significant figures depending upon the total temperature of the receiver cooling water.

It should also be noted that small variations in flux did occur very rapidly during the operation of the arc-image furnace. The cause of these fluctuations is believed to be the physical condition and age of the carbon electrodes. These electrodes were produced in mass quantities for the sole purpose of illumination, therefore, small imperfections in the composition were of no consequence at that time. No determination of the amount of deterioration of the electrodes has been made, and no suitable method for analysis is apparent, however, it is known by the packaging date of 1942 that the age of the electrodes is approximately 18 years. It logically seems that the performance of the electrodes would be reduced with age. No information is available, however, to support this hypothesis.

An equivalent blackbody temperature, T_b , which is the temperature of a perfect emitter necessary to produce the radiation flux measured by the calorimeter, was defined for this thesis as:

$$T_b = \left(\frac{Q}{\sigma}\right)^{1/4}$$

where: Q = radiation flux

σ = Stefan-Boltzmann constant

This relation is a re-arrangement of the Stefan-Boltzmann relation, $Q = T^4$, the thermal radiation produced by a blackbody at the absolute temperature T . A range of equivalent blackbody temperatures from 2500°R at the base position to 5300°R at the optimum point was determined from the radiation flux and given in Table III. The range of equivalent blackbody temperatures for the various flux distribution test positions

is also shown graphically in Fig. 22.

One significant observation made during the flux distribution test series was that regardless of the calorimeter position, the heat absorption by the reflector was essentially constant. No information is available with which this effect can be compared. The author, therefore, can only theorize the cause for such an occurrence.

The solid angle of the calorimeter was constructed equal to the solid angle of the furnace reflectors, therefore, at the focal plane or optimum point of radiation flux a small portion of the intense radiation is striking the reflector. Then, as the reflector is being withdrawn, an amount of radiation inversely proportional to the reduction in radiation flux at any position compared to the radiation flux at the optimum point, more directly strikes the reflector. This combination of a reduction in intensity with an increase in radiation contacting the reflector appears to be the most logical conclusion which can be formulated as to the cause of a constant absorption of heat by the calorimeter reflector regardless of position.

Other Pertinent Information From all Test Series

One item of primary importance from the beginning of this thesis was the performance of the arc-image furnace. Much work and many operating difficulties had been anticipated because the two search lights which form the arc-image furnace had been taken out of storage, cleaned, stripped of unnecessary wiring and controls, and put into operation in approximately one year. However, after a few minor troubles being corrected, the arc-image furnace performed quite satisfactorily in that

the arc voltage and current remained at essentially constant values. It has been previously stated that small variations in the radiation flux produced by the arc-image furnace did occur due to the condition of the electrodes. It is felt however that as long as flow rates, approximately equal to those used in this investigation, are employed, the small variations in radiation flux will not be detected by the instrumentation. This is due to the fact that the response of the large thermal mass is too slow to indicate small fluctuations.

It had been hoped prior to the flux distribution test series that equivalent blackbody temperatures approaching 6000°R would be produced. Upon visual inspection of the reflector, it is clearly noticeable that the surface of the cylindrical portion of the aperture does not exhibit as smooth a surface and as high a reflectivity as desired. Since the heat absorption of the reflector is very large, it is quite probable that a large amount of heat, which should be reflected into the calorimeter receiver, is being undesirably absorbed in this portion of the reflector. If the amount of undesirable heat absorption could be determined, corrections could be made which would elevate the equivalent blackbody temperature.

Another consideration which would elevate equivalent blackbody temperatures is the effect of the receiver's actual absorptivity. Although it is theorized that the actual absorptivity of the permanent receiver approaches unity, no instrumentation is available by which the actual absorptivity of the receiver can be determined. If the actual absorptivity of the calorimeter is significantly less than unity, cor-

rections to the radiation flux would further elevate equivalent black-body temperatures.

To give an estimate of the overall transfer of heat of the arc-image furnace, a combined efficiency should be considered. For this thesis the combined efficiency, η_c , is defined as the ratio of the total heat absorbed by the calorimeter to the heat equivalent of electrical power released in the arc, or in equation form,

$$\eta_c = \frac{(q_T) (1000) (60)}{(V) (C) (3413)}$$

where: q_T = estimated total heat absorbed

V = arc voltage

C = arc current

The total heat absorbed by the calorimeter is vastly reduced as the calorimeter is moved from the optimum point. For that reason, only the combined efficiency at the optimum point is considered. The total heat absorbed by the calorimeter is approximately 45 Btu/min with the arc-image furnace operating at an arc voltage of 78 volts D.C. and an arc current of 150 amperes. These values render a combined efficiency of 6.8%.

A low efficiency is to be expected for several reasons, foremost of which is the fact that the geometrical configuration of the furnace allows only 25% of the radiation being produced by the arc to be collected by the sending furnace reflector. As the radiation travels to the receiving reflector and then to the calorimeter, obstacles such as the arc-shield, arc-shield support and control rods block an unknown portion of radiation. The radiation is further reduced by the physical condition of reflective surface on the furnace reflectors and the deviation of the reflector from

the ideal parabolic configuration. Finally, an unknown portion of radiation is absorbed by water vapor and carbon dioxide in the atmosphere.

Considering that 25% is the optimum combined efficiency possible, the efficiency of the arc-image furnace and calorimeter is apparently good when the limitations of the installation are taken into account. It must be noted, however, that no published data is available which a comparison of efficiencies can be made.

In concluding the discussion, the author feels that this investigation was highly successful and highly informative.

VI. CONCLUSIONS

As a result of the investigation completed, the following conclusions have been formulated.

1. The operation of the arc-image furnace is quite satisfactory.
2. Receiver number one theorized as having the best absorptivity of the three receivers tested, actually did have the highest absorptivity at all test positions.
3. The heat absorption of the reflector is sufficiently large to be causing the radiation flux, as measured by receiver, to appear much lower than it actually is.
4. The heat absorption of the reflector is essentially constant regardless of the calorimeter position.
5. The equivalent blackbody temperature existing at the optimum point is lower than equivalent blackbody temperature that was desired from the apparatus.
6. The combined efficiency of the furnace and calorimeter although apparently low, is acceptable.

VII. RECOMMENDATIONS

It is felt by the author that to more readily adapt the calorimeter developed in this thesis for high temperature research, a study of the heat absorption by the reflector should be made.

It would also be advisable to study the possibility of utilizing higher power input to the arc in order to produce larger quantities of radiation flux at the focal plane of the furnace receiving reflector.

For use of the apparatus in the investigation of specimens under various values of radiation flux, a control device should be developed and installed.

It is felt that at the present stage of development, the arc-furnace and the calorimeter could be applied to investigate the absorptivity of various gases.

It is felt that a calibrated radiometer should be obtained, and a determination made of the actual flux existing at various positions within the arc-image furnace, thus enabling a calibration of the calorimeter to be made.

It is recommended that, for stability, some additional means of securing the furnace reflectors should be devised and installed.

In order to facilitate easier operation of the calorimeter, it is recommended that a water line be installed in the immediate area of the arc-image furnace.

VIII. ACKNOWLEDGEMENTS

This thesis would have been impossible had it not been for the generous assistance and support which was given the author by many individuals.

To Professor R. K. Will, head of the thesis committee, to Doctor H. L. Wood and to Professor A. J. Metzger, members of the thesis committee, the author feels sincerely appreciative for the aid, advice, constructive criticism, and interest that have extended in the production of this thesis.

To Professor J. B. Jones, Head of the Department of Mechanical Engineering, the author would like to express his appreciation for the opportunity of studying in his department.

To Professors C. H. Long and H. S. Miles, Jr., the author would like to offer his thanks for the aid given during the preparation of this thesis.

To the other members of the Mechanical Engineering staff, the author would like to offer thanks for the moral support which was given.

To Messrs. H. M. Smith and F. H. Grissom, the author would like to give special thanks for the fabrication of vital mechanical components used in this thesis.

To Messrs. C. E. Pond and T. E. Boggess of The Norfolk and Western Railway Company, the author would like to offer his appreciation for the assistance they extended in having the calorimeter reflector ni-chrome plated.

To Nancy, his wife, for her support, understanding, patience and assistance throughout the entire production of this thesis, the author is eternally indebted.

IX. BIBLIOGRAPHY

1. AREF, M. N., "Emissivity Measurement of Industrial Surfaces due to Thermal Radiation," ASME paper No. 58-HT-18; June, 1958, pp. 8-14.
2. BAKER, H. D., RYDER, E. A. and BAKER, N. H., Temperature Measurement in Engineering, Vol. I, Chapter 2, pp. 16-18; John Wiley and Sons, New York, 1953.
3. BIRKEBAK, R. C., The Experimental Determination of The Total Absorptivity of Several Important Engineering Materials for Solar Radiation, Master's Thesis, University of Minnesota, pp. 1-33, September, 1956.
4. BIRKEBAK, R. C. and HARTNETT, J. P., "Measurements of the Total Absorptivity for Solar Radiation of Several Engineering Materials", ASME paper No. 57-SA-27, pp. 1-3; March, 1957.
5. COBLENTZ, W. W., National Bureau of Standards Bulletin, "The Diffuse Reflecting Power of Various Substances", Vol. 9, 1913.
6. COHEN, R. K., and HIESTER, N. K., The Journal of Solar Energy Science and Engineering, "A Survey of Solar Furnace Installations in the United States", Vol. 1, April-July, 1957, pp. 115-117.
7. CONN, W. M., High Temperature Technology, "Obtaining Very High Temperatures by Solar Furnaces", pp. 319-326; John Wiley and Sons, New York, 1956.
8. CORBINE, J. D. and WILBUR, D. A., High Temperature Technology, "The Electrical Torch", pp. 327-330.
9. Correspondence with COOMBS, G. D., Research Equipment Engineer, Arthur D. Little, Inc., November, 1959.
10. DIKE, P. H., High Temperature Technology, "Pyrometry by Radiation Methods", pp. 335-353; John Wiley and Sons, New York, 1956.
11. DOBBINS, J. P., "Emittance of Oxidized Metals", ASME paper No. 50-A-58, Annual Meeting 1950, pp. 2-22.
12. DUNKLE, R. V. and GIER, J. T., "Thermal Radiation Project", Institute of Engineering Research, University of California, Final Report, pp. 99-104; September, 1950

13. ECKERT, E. R. G., HARTNETT, J. P. and IRVINE, T. F., Jr.,
"Measurement of Total Emissivity of Porous Materials In Use
for Transpiration Cooling", Jet Propulsion, Vol. 26, pp. 280-
281.
14. ECKMAN, D. P., Industrial Instrumentation, Chapter 5, pp. 127-150;
John Wiley and Sons, New York, 1960.
15. EYERLY, G. B. and LAMBERTON, W. A., High Temperature Technology,
"Development and Operation of a Quenching Furnace for Temp-
eratures of 1500-2800°C", pp. 259-263; John Wiley and Sons,
New York, 1956.
16. EYERLY, G. B. and LAMBERTON, W. A., High Temperature Technology,
"High Temperature Induction Heat Treatment of Readily
Oxidized Metals", pp. 268-270; John Wiley and Sons, New
York, 1956.
17. FISHER, H., Conference on Extremely High Temperatures, "Upper
Temperature Limits in the High Pressure Discharge", pp. 11-29;
March, 1958.
18. GELLER, R. F., High Temperature Technology, "The Oxide Resistor
Furnace", pp. 263-268; John Wiley and Sons, New York, 1956.
19. GLASER, P. E., The Journal of Solar Energy Science and Engineering,
"A Solar Furnace for use in Applied Research", Vol. 1, April-
July, 1959, pp. 63-67.
20. GLASER, P. E., Review of Scientific Instruments, "High Radiation-
Flux, Absolute, Water Flow Calorimeter", Vol. 28, No. 12,
pp. 1084-1086; December, 1957.
21. HOGE, H. J., Temperature, It's Measurement and Control in Science
and Industry, "Temperature Measurement in Engineering",
Vol. II, Chapter 18, pp. 287-323; Reinhold Publishing Co.
22. HUTCHINS, American Journal of Science, Vol. 6, 1898, pp. 373.
23. IRVINE, T. F., Jr., HARTNETT, J. P. and ECKERT, E. R. G., "Total
Normal Emissivities Measurements for Porous Materials Used
for Mass-Transfer Cooling", ASME paper No. 57-F-8, pp. 1-5;
May, 1957.
24. IRVINE, T. F., Jr., HARTNETT, J. P. and ECKERT, E. R. G., Solar
Collector Surfaces With Wave Length Selective Radiation
Characteristics, Publication of Heat Transfer Laboratory,
Mechanical Engineering Department, University of Minnesota,
pp. 12-16.

25. JAKOB, M., Heat Transfer, Vol. I and Vol. II, General Reference, John Wiley and Sons, New York, 1949, 1957.
26. JANES, G. S. and PATRICK, R. M., Conference on Extremely High Temperatures, "The Production of High Temperature by Magnetic Acceleration", March 1958, pp. 3-10.
27. McADAMS, W. H., Heat Transmission, General Reference, 3rd Edition, McGraw-Hill Book Company, New York, 1954.
28. METZGER, J. W., The Measurement of Infrared Emissivities of Metals at Elevated Temperatures, Master's Thesis, Drexel Institute of Technology, pp. 1-73; June, 1959.
29. NEWHALL, H. S. and LEE, J. R., High Temperature Technology, "Consideration in the Design of Electric Arc-Furnaces for High-Temperature Work", pp. 278-287.
30. Publications of Arthur D. Little, Inc., "ALD-Strong Arc Imaging Furnace", September, 1959.
31. SHERWOOD, E. M., High Temperature Technology, "Means of Achieving High Temperatures and Some of Their Limitations", pp. 251-256; John Wiley and Sons, New York, 1956.
32. STEVEN, G., "High Temperature Thermocouples", High Temperature Technology, pp. 357-365; John Wiley and Sons, New York, 1956.
33. THRING, M. W., The Science of Flames and Furnaces, Chapter 2, pp. 88-90; John Wiley and Sons, New York, 1952.
34. WILKES, G. B., Measurements of the Total Normal Emissivity of Materials, Progress Report, No. 9, Massachusetts Institute of Technology.
35. TUDDENHAM, W. M., The Journal of Solar Energy Science and Engineering, "A Solar Furnace For Research in Non-Ferrous Metallurgy, Vol. 1, April-July, 1957, pp. 48-57.
36. WOOD, W. P. and CORK, J. W., Pyrometry, 2nd Edition, Chapter 3, 5 and 6, pp. 33-53, 103-168; McGraw-Hill Book Company, New York, 1941.
37. WORTHING, A. G., Temperature, It's Measurement and Control in Science and Industry, "Temperature Radiation Emissivities and Emittances" pp. 1164-1186, Reinhold Publishing Company, New York, 1941.

X. APPENDIX

The appendix for this investigation consists of a calibration curve for the copper-constantan thermocouples employed in the determination of various temperatures.

Electromotive Force, mV

0.78

0.76

0.74

0.72

0.70

68.0

2

4

6

8

65.0

2

4

6

8

66.0

2

4

6

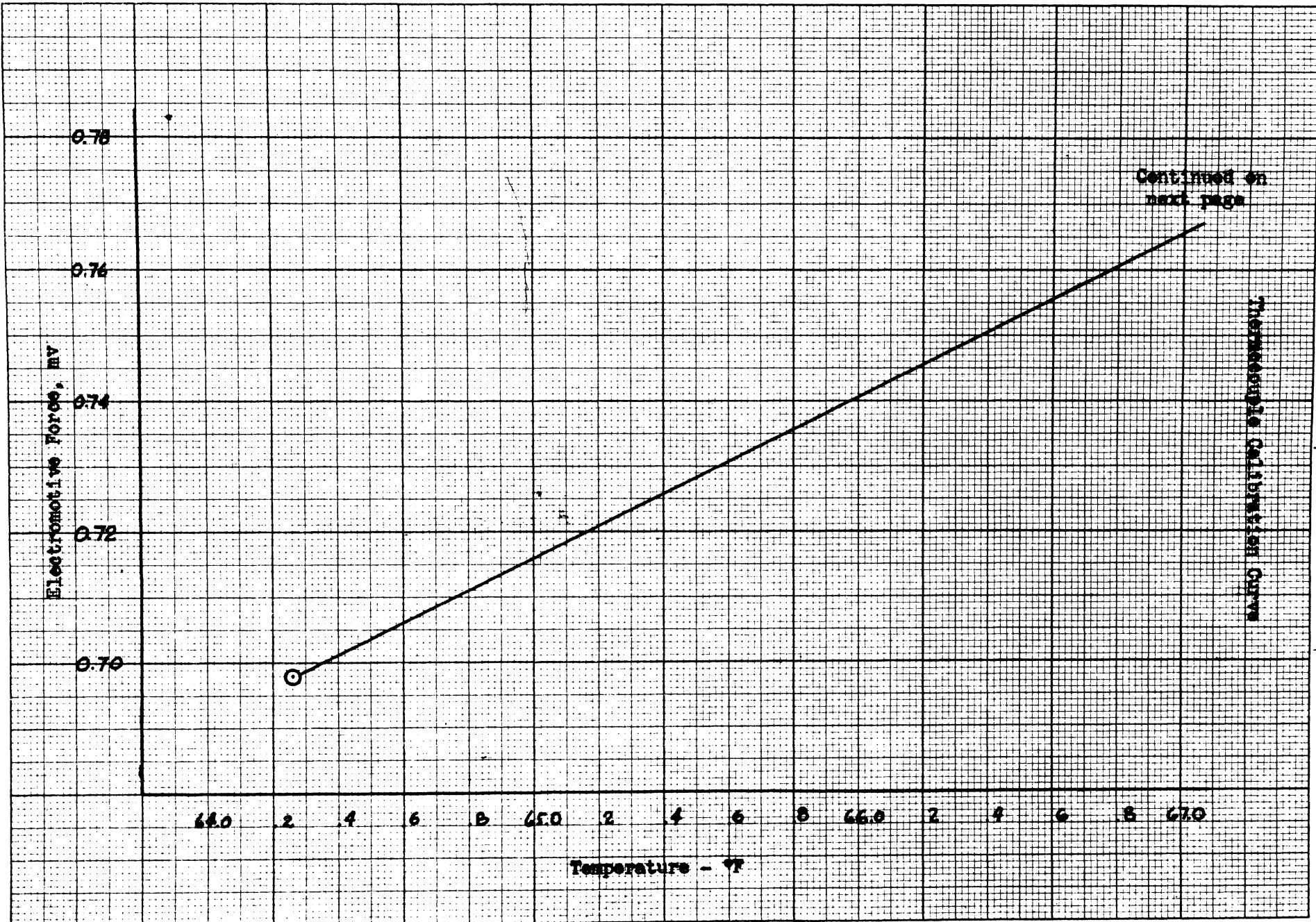
8

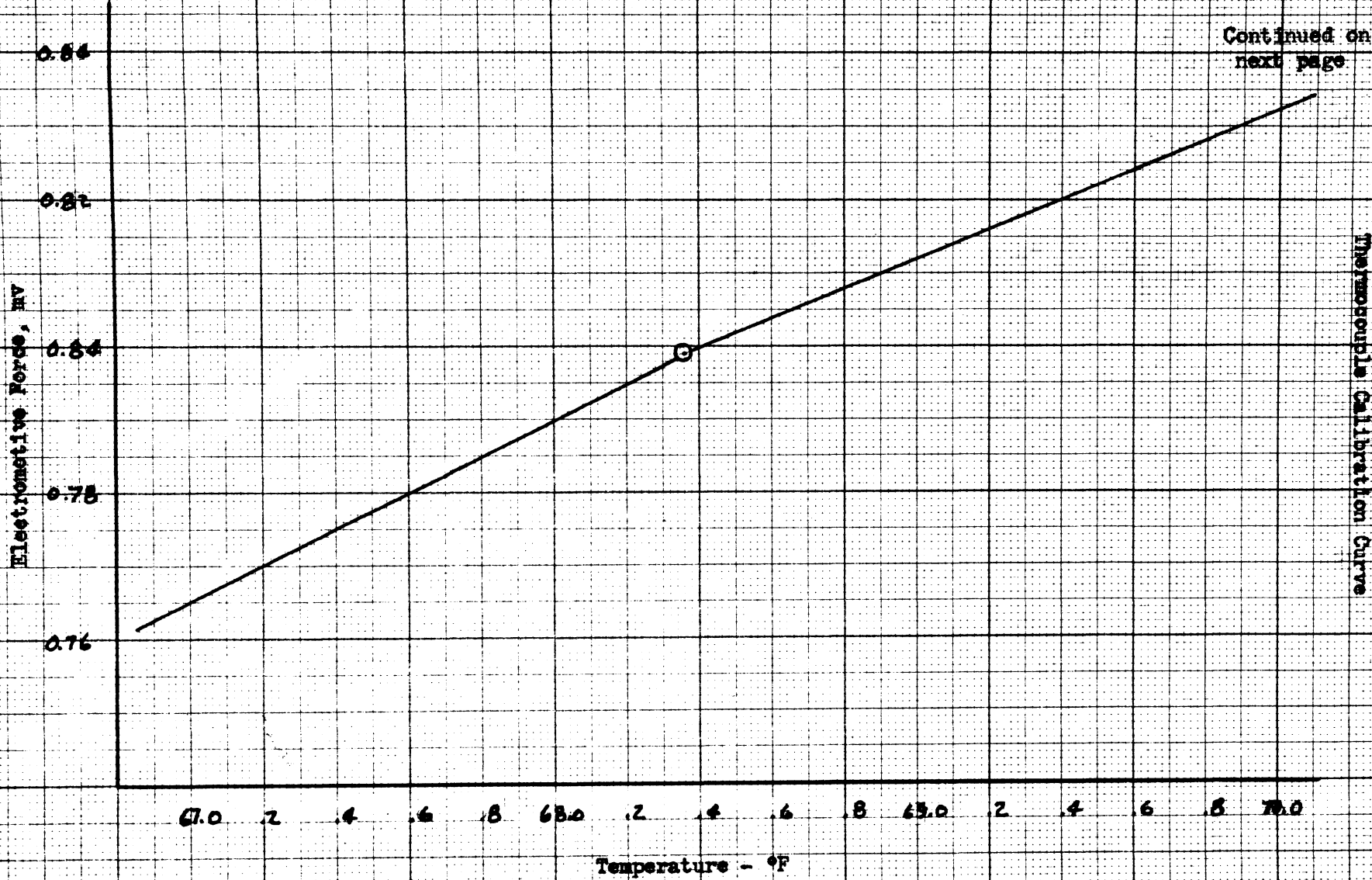
67.0

Temperature - °F

Continued on
next page

Thermocouple Calibration Curve





Thermocouple Calibration Curve

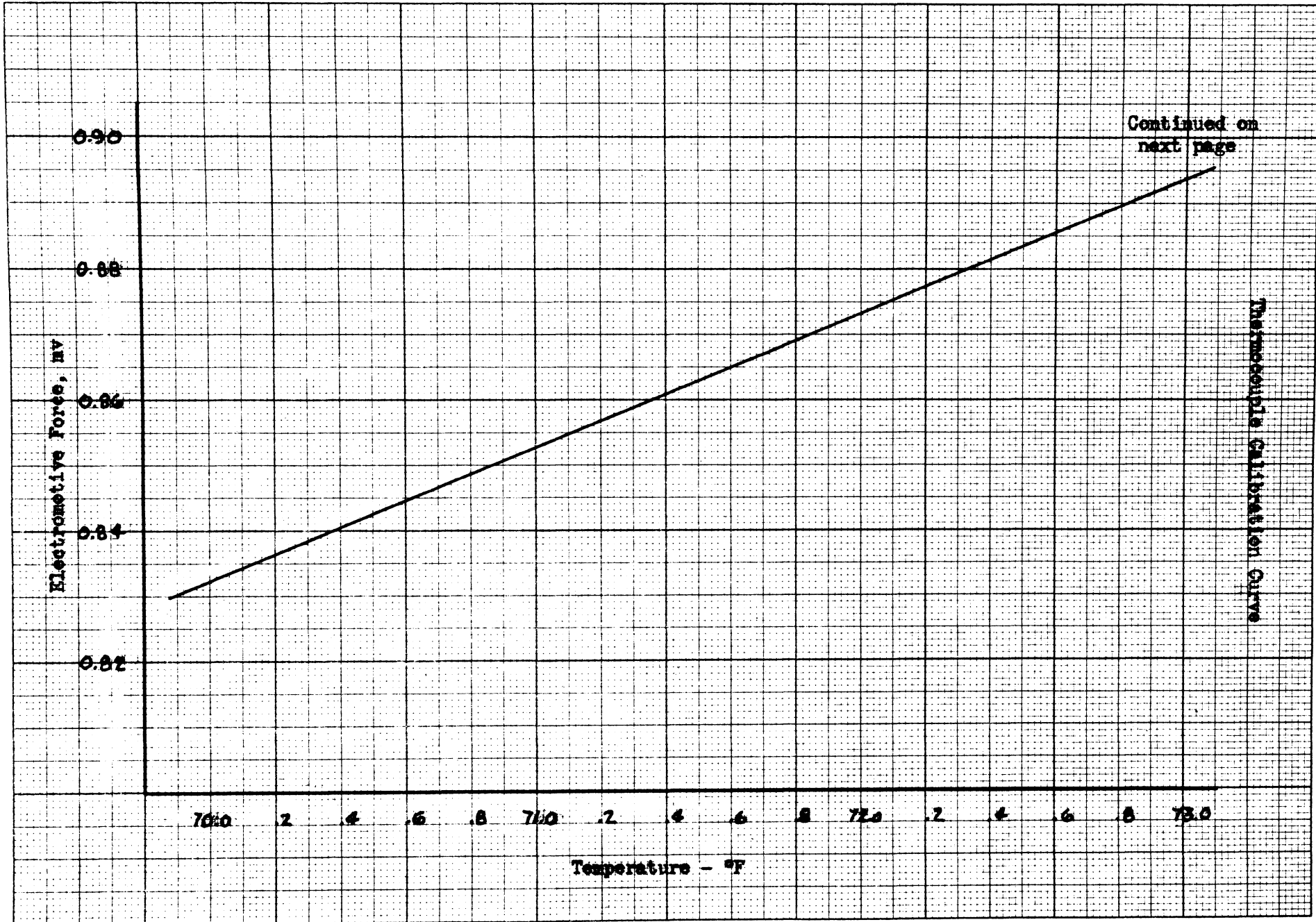
Electromotive Force, mv

70.0 2 4 6 8 71.0 2 4 6 8 72.0 2 4 6 8 73.0

Temperature - °F

Continued on
next page

Thermocouple Calibration Curve

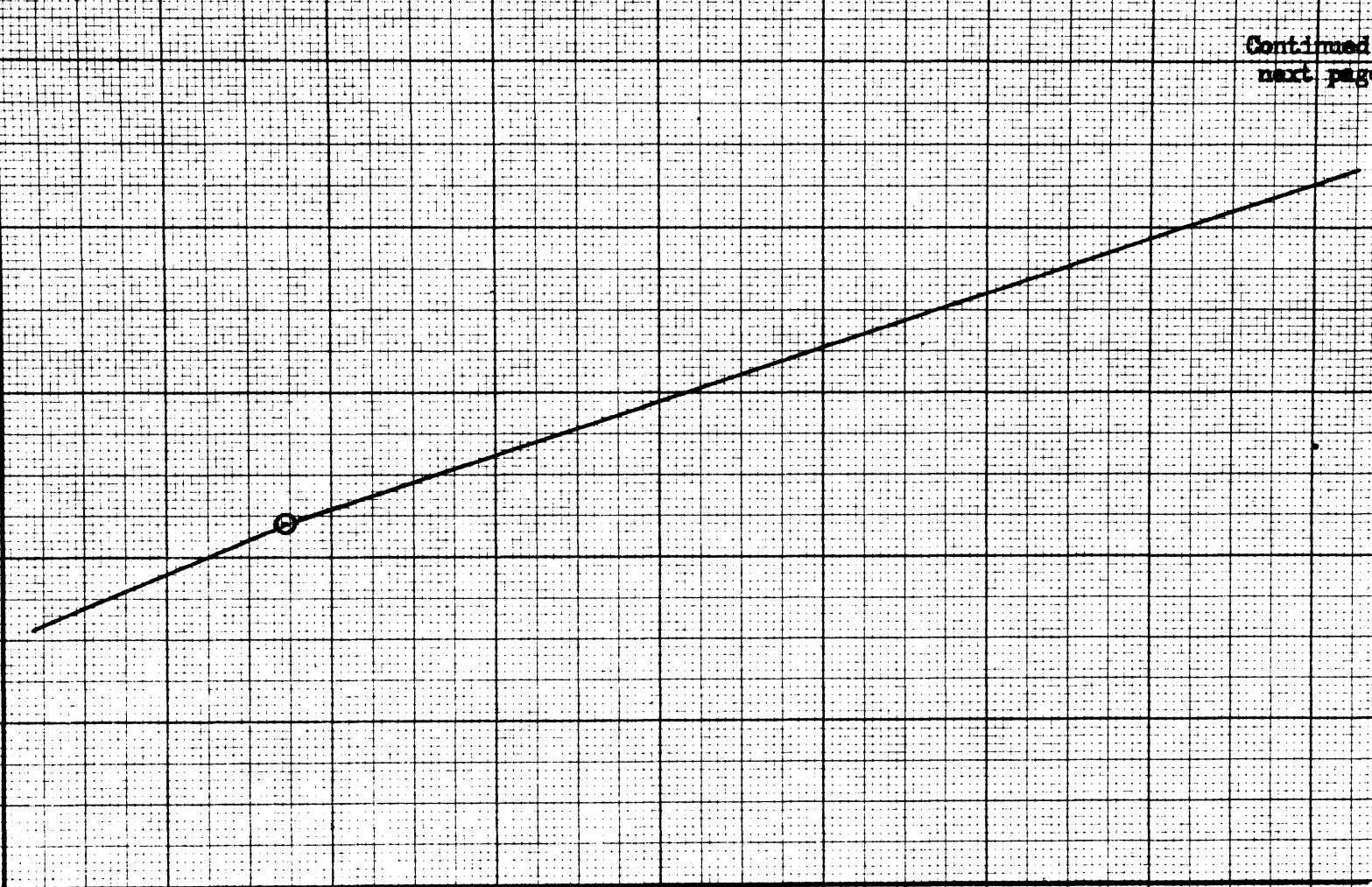


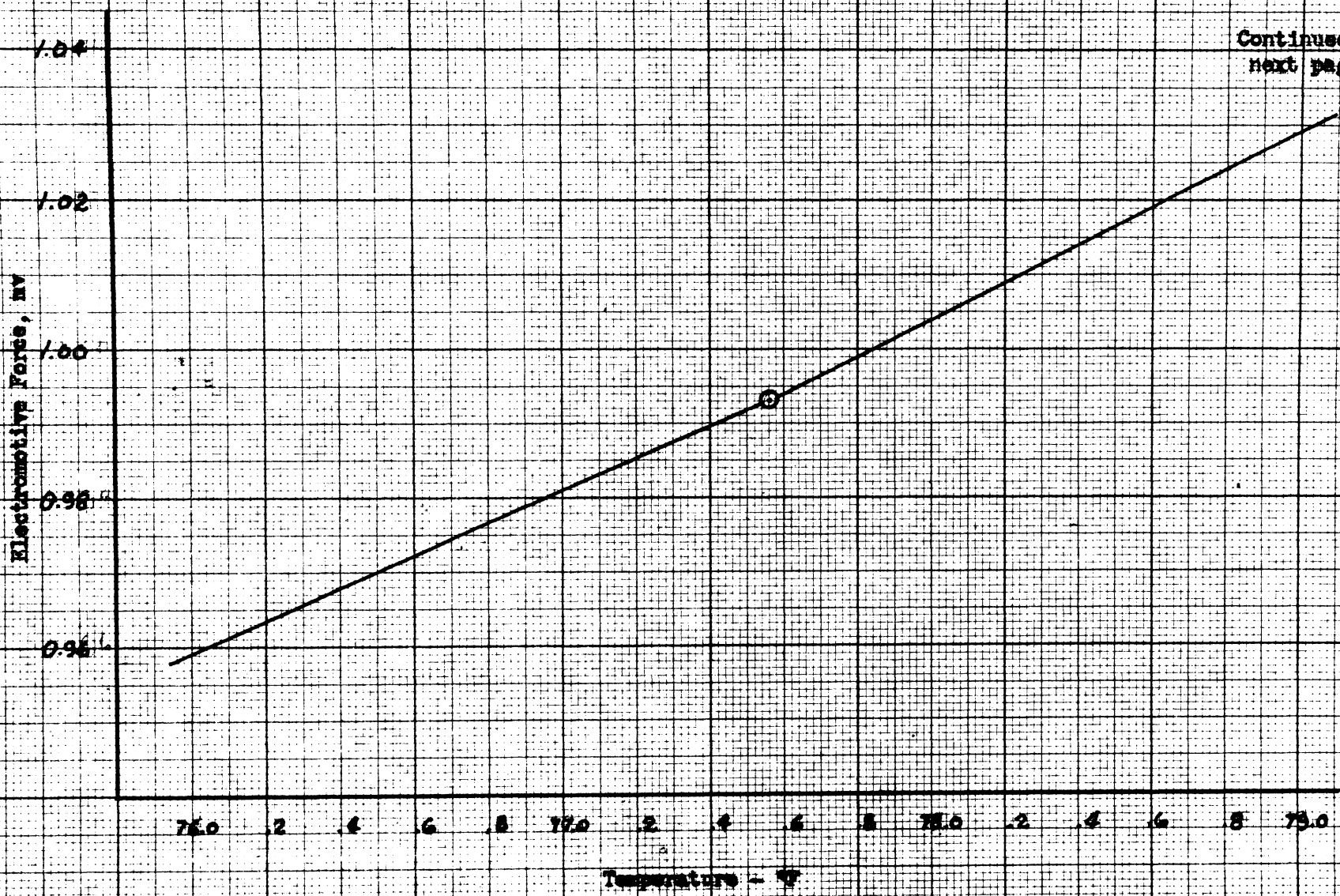
Continued on
next page

Electromotive Force, mV

Thermocouple Calibration Curve

Temperature - °F





Continued on
next page

Thermocouple Calibration Curve

Electromotive Force, mv

1.12

1.10

1.08

1.06

1.04

Continued on
next page

Thermocouple Calibration Curve

79.0

.2

.4

.6

.8

800

.2

.4

.6

.8

810

.2

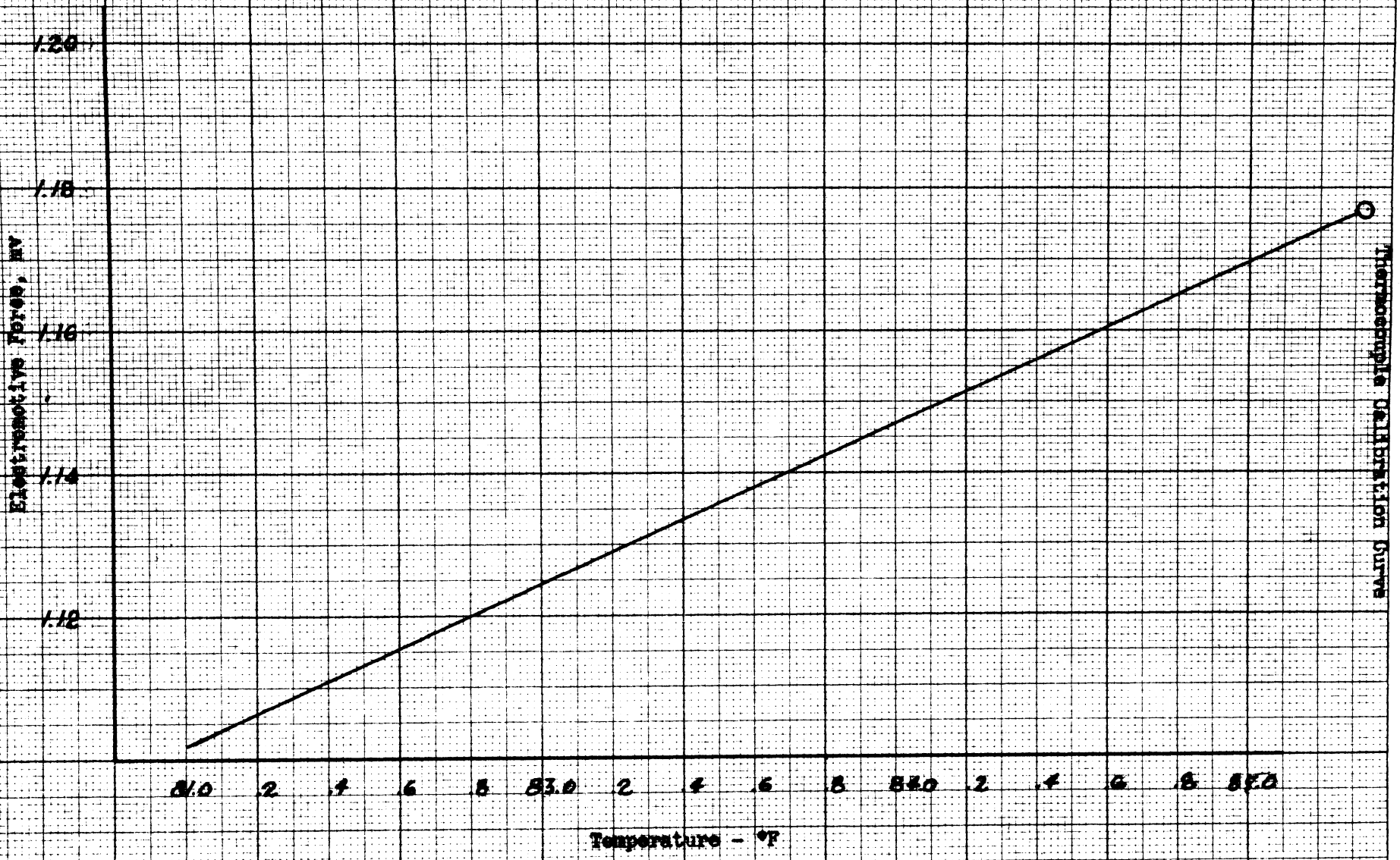
.4

.6

.8

820

Temperature - °F



Thermocouple Calibration Curve

**The vita has been removed from
the scanned document**

ABSTRACT

The object of this investigation was to determine the optimum receiver configuration to be used in an absolute, high radiation flux, calorimeter.

Three receivers of different configuration were designed, fabricated, and tested in an arc-image furnace. The results proved conclusively that the optimum receiver configuration was cylindrical with a radial entrance.

The receiver was employed in determining that the performance of the calorimeter is independent of cooling water flow rates.

The calorimeter was also used to study the flux distribution of the arc-image furnace in the Mechanical Engineering Department. The radiation flux at the optimum point of the arc-image furnace, as measured by the calorimeter, was determined to be 1.35×10^6 Btu/hr-ft². Considering the area of the calorimeter aperture, this radiation flux corresponds to an equivalent blackbody temperature of 5300°R.